Multifractal formalisms for multivariate analysis

Stéphane Jaffard[1], Stéphane Seuret[1], Herwig Wendt[2], Roberto Leonarduzzi[3,4], and Patrice Abry[4]

[1]Université Paris-Est, LAMA (UMR 8050), UPEM, UPEC, CNRS, Créteil, France
[2]Université de Toulouse, CNRS, IRIT, Toulouse, France
[3]Ecole Normale Supérieure, PSL, 75005, Paris, France
[4]Université de Lyon, ENS de Lyon, Université Claude Bernard, CNRS, Laboratoire de Physique, Lyon, France

Multifractal analysis, that quantifies the fluctuations of regularities in time series or textures, has become a standard signal/image processing tool. It has been successfully used in a large variety of applicative contexts. Yet, successes are confined to the analysis of one signal or image at a time (univariate analysis). This is because multivariate (or joint) multifractal analysis remains so far rarely used in practice and has barely been studied theoretically: In view of the myriad of modern real-world applications that rely on the joint (multivariate) analysis of collections of signals or images, univariate analysis constitutes a major limitation. The goal of the present work is to theoretically ground multivariate multifractal analysis by studying the properties and limitations of the most natural extension of the univariate formalism to a multivariate formulation. It is notably shown that while performing well for a class of model processes, this natural extension is not valid in general. Based on the theoretical study of the mechanisms leading to failure, we propose alternative formulations and examine their mathematical properties.

THE ROYAL SOCIETY
PUBLISHING

1. Introduction

• **Context: Multifractal Analysis.** Multifractal analysis consists in analyzing functions, signals, images, sample paths of stochastic processes, random or deterministic measures by quantifying the size of sets of points in $\mathbb{R}^d$ sharing a same singularity exponent H. Theoretically, multifractal analysis amounts to computing the *multifractal spectrum* $D(H)$, which encapsulates the Hausdorff dimensions of the sets of points where a pointwise regularity exponent takes a given value H. Practically, Hausdorff dimensions cannot be estimated from real-world data. Instead, an indirect estimation of $D(H)$ that can actually be computed from data, a so-called *multifractal formalism*, is used: The estimate is obtained by computing a *Legendre spectrum*. For univariate data (single signal, image,...), the Legendre spectrum has been shown to yield an upper bound for $D(H)$ [1], and to coincide with $D(H)$ for several models of deterministic functions or stochastic processes commonly used to model scale-free dynamics (cf. e.g., [2] and ref. therein). Thus, the derivation of multifractal formalisms yielding appropriate Legendre spectra, i.e., spectra that are both as close as possible to $D(H)$ and remain practically computable, is a central issue.

Multifractal analysis and modeling have been widely used and have led to significant successes in several applications very different in nature (cf. e.g., [2–4] and ref. therein). Yet, these achievements were mostly obtained in a univariate setting: One signal or image is analyzed at a time and independently of others. Such analyses miss potentially crucial information coded in cross-dependencies. However, in most recent applications, systems are monitored through large collections of signals or images recorded simultaneously. This critically calls for the theoretical definition and study of multivariate multifractal analysis and the development of multivariate multifractal formalisms, at the heart of the present work.

• **Related work: Multivariate multifractal analysis.** Multifractal analysis was historically grounded in the study of hydrodynamic turbulence [5]. Therefore, the notion of multivariate multifractal analysis was first introduced in that context as a *natural* extension of the univariate formalism [6]. Multivariate multifractal analysis was then theoretically studied in an abstract setting in [7] and in specific cases: Several pointwise exponents associated with invariant measures of expanding dynamical systems (level sets of Birkhoff averages, pointwise dimensions, local entropies, and Lyapunov exponents) are considered in [8]; as regards the usual local dimension, general results for doubling measures are obtained in [9], and selfsimilar measures associated with an IFS satisfying the Open Set Condition are studied in [10,11]; see also [12]. However, multivariate multifractal analysis remained used only in rare occasions on real-world data, cf. e.g. [13] and references therein. This is mostly due to a lack of theoretical understanding of the information encoded in mutivariate spectra and of theoretical constructions for mutifractal formalisms, as well as to a lack of efficient and robust practical analysis tools. Several theoretical issues underlying multivariate multifractal analysis were recently investigated in [9,13–15], and the present paper is a continuation of these works. Further, the potential interests of the multivariate Legendre spectrum to study real-world data were investigated in [16,17], together with the definition of bivariate log-cumulants (a mandatory step for an efficient practical implementation of multivariate multifractal analysis).

• **Goals, contributions and outline.** The main goals of the present paper are: 1) to discuss the mathematical foundations of the seminal proposition of a multivariate multifractal formalism in [6], 2) to understand its range of validity and 3) to identify the origin of its limitations and propose theoretical solutions to overcome them. To that end, Section 2 starts by stating in a multivariate setting the mathematical notions (pointwise regularity and multifractal spectrum) attached to multifractal analysis. It further discusses the issues at hand in the computation of the dimensions of intersections of fractal sets, which turn crucial in a multivariate setting.

Section 3 motivates the wavelet leader based reformulation of the multivariate multifractal formalism proposed in [6] and establishes the theoretical conditions under which this formalism is valid. This requires to revisit the relationships between multiscale quantities (e.g., wavelet leaders) and pointwise regularity (e.g., Hölder exponent) and to put into light the key notion of

compatibility; additionally, it leads to the introduction of a new notion in multivariate multifractal analysis: *synchronicity* between the *minimizing sequences* of multiscale quantities associated with each of the different components of the data. It will allow to establish the required conditions under which the multivariate Legendre spectrum provides an upper bound for the multivariate multifractal spectrum.

Since multiplicative cascades constitute the paradigm for multifractal construction, elaborating on [6,9,10,13], Section 4 studies in depth bivariate deterministic dyadic binomial cascades. It establishes analytically their multivariate Legendre spectra, thus complementing [13] where their multifractal spectra were determined. These results show that the currently available formalism proposed in [6] does not necessarily yield an upper bound for the multifractal spectrum: This critically depends on whether minimizing sequences of multiscale quantities associated with cascades satisfy or not the *synchronicity* requirement.

Section 5 elaborates other examples of bivariate processes (bivariate scale-lacunary wavelet series and bivariate independent Lévy processes) for which the multivariate Legendre spectrum does not provide an upper bound for the multivariate multifractal spectrum and lays bare the mechanisms leading to failure. They suggest an alternative, a *cross-scale* multivariate multifractal formalism, of which we lay the theoretical foundations and study the general validity.

Section 6 discusses potential interpretations of the multivariate multifractal and Legendre spectra in relation to synchronicity vs. non synchronicity and statistical dependencies vs. independence.

The theoretical developments proposed in this work are supported by practical illustrations of the actual numerical implementation of multivariate formalisms, obtained from a toolbox that will be made publicly and freely available in a documented manner at the time of publication.

2. Multivariate multifractal analysis: Intuitions and definitions

(a) Pointwise regularity

Let $X(x) = (X_1(x), \cdots , X_M(x)), x \in \mathbb{R}^d, X \in \mathbb{R}^M$, denote either a multivariate deterministic function or the multivariate sample path of a stochastic process. In essence, the multifractal analysis of X consists in characterizing the fluctuations along x of local or *pointwise regularity* indices of X, also termed *singularity* indices, and hereafter denoted $h(x) = (h_1(x), \cdots , h_M(x))$. These indices measure roughness of X around location x, independently for each component X_k.

A widely used regularity index is the *Hölder exponent*, $h_f(x_0)$ of f at $x_0 \in \mathbb{R}^d$. For a univariate locally bounded function $X_k : \mathbb{R}^d \to \mathbb{R}$ it is defined as follows: For $\alpha \geq 0$, $X_k \in C^\alpha(x_0)$ if there exist a constant $C > 0$ and a polynomial P of degree less than α such that, for ϵ small enough,

$$\sup_{|x-x_0| \leq \epsilon} |X_k(x) - P(x - x_0)| \leq C\epsilon^\alpha, \tag{2.1}$$

then $h_{X_k}(x_0) = \sup\{\alpha \geq 0 \mid X_k \in C^\alpha(x_0)\}$. Other indices are used to quantify regularity. For example, for nonnegative measures μ, the *lower and upper local dimensions* are defined as:

$$\ell_\mu^-(x_0) = \liminf_{\rho \to 0^+} \frac{\log \mu([x_0 - \rho, x_0 + \rho])}{\log \rho} \quad \text{and} \quad \ell_\mu^+(x_0) = \limsup_{\rho \to 0^+} \frac{\log \mu([x_0 - \rho, x_0 + \rho])}{\log \rho}, \tag{2.2}$$

and for non locally bounded functions, p-exponents replace and generalize the Hölder exponent, cf. [3,4]. Further, to enrich the description of local regularity provided by such indices, the use of *lacunarity, cancellation* and *oscillation* exponents, was proposed, cf. [18] and references therein. Any of these pointwise regularity indices can be used in the following.

(b) Multivariate multifractal spectra: Definitions and properties

A fundamental postulate of multifractal analysis is that the relevant information on X is not given by the local evolution of $h(x)$ as a function of x but that it is encoded *globally* and *geometrically*, in form of the fractal (Hausdorff) dimensions of well-chosen level sets of singularity indices.

Several types of (univariate or multivariate) sets can be considered: For $H = (H_1, \ldots, H_M)$,

$$\forall m = 1, \ldots M, \qquad E_m(H_m) = \{x \in \mathbb{R}^d : h_m(x) = H_m\},$$

$$E(H) = \{x \in \mathbb{R}^d : h_1(x) = H_1, \ldots, h_M(x) = H_M\}, \qquad (2.3)$$

$$E^{\geq}(H) = \{x \in \mathbb{R}^d : h_1(x) \geq H_1, \ldots, h_M(x) \geq H_M\}, \qquad (2.4)$$

$$E^{\leq}(H) = \{x \in \mathbb{R}^d : h_1(x) \leq H_1, \ldots, h_M(x) \leq H_M\}. \qquad (2.5)$$

By definition, the multivariate singularity sets consist of intersections of univariate ones:

$$E(H) = E_1(H_1) \bigcap \ldots \bigcap E_M(H_M). \qquad (2.6)$$

For large classes of deterministic functions or sample paths of stochastic processes, such sets are fractal. Their sizes, as functions of H, referred to as *multivariate multifractal spectra*, are thus informatively quantified by their Hausdorff dimension, denoted $\dim$:

$$D(H) = \dim(E(H)), \quad D^{\geq}(H) = \dim(E^{\geq}(H)), \quad \text{and} \quad D^{\leq}(H) = \dim(E^{\leq}(H)). \qquad (2.7)$$

By convention, $\dim(\emptyset) = -\infty$. Though theoretical results in multifractal analysis are often stated in terms of $D(H)$ only, the other two spectra, $D^{\geq}(H)$ and $D^{\leq}(H)$, also play key roles. For instance, in univariate settings where multifractal spectra usually satisfy $D^{\leq}(H) = \sup_{H' \leq H} D(H')$ and $D^{\geq}(H) = \sup_{H' \geq H} D(H')$, the strongest versions of upper bounds for spectra are stated in terms of $\mathcal{D}^{\geq}(H)$ and $\mathcal{D}^{\leq}(H)$, and the determination of $D(H)$ requires such stronger estimates as a prerequisite. More conceptually, the sets $E^{\geq}(H)$ and $E^{\leq}(H)$ often are simpler to describe mathematically than $E(H)$, and their properties are better understood.

Multivariate multifractal spectra satisfy a number of properties. By definition $E(H)$ is included in any of the $E_k(H_k)$, thus yielding

$$\forall H = (H_1, \ldots H_M), \quad D(H) \leq \min(D_1(H_1), \ldots, D_M(H_M)). \qquad (2.8)$$

The *support* of the spectra, $\mathcal{S}upp(D) = \{H : E_H \neq \emptyset\} = \{H : D(H) \geq 0\}$, satisfies

$$\mathcal{S}upp(D) \subset \mathcal{S}upp(D_1) \times \ldots \times \mathcal{S}upp(D_M).$$

Since $E_1(H_1) = \bigcup_{H_2, \ldots, H_M} E(H_1, H_2, .., H_M)$, we have $D_1(H_1) \geq \sup\limits_{H_2, .., H_M} D(H_1, H_2, ..., H_M)$ (similar formulas are true for the other coordinates $D_k(H_k)$). Equality may fail because the union is taken on a non-countable set, but for many multifractal models, equality holds (see Section 4).

(c) Intersection of fractal sets

While the properties of spectra in univariate settings have been widely studied, those of multivariate spectra remain barely investigated. A key issue is to understand which information the shape of the multivariate multifractal spectrum yields on *dependencies* between components. A first extreme case consists of all components being identical ; then the multivariate multifractal spectrum $D(H)$ is supported by the diagonal $H_1 = \ldots = H_M$ and coincides with the univariate spectra $D_1(H_1) = \ldots = D_M(H_M)$. But in general, obtaining multivariate multifractal spectra amounts to computing the Hausdorff dimensions of intersections of fractal sets, cf. (2.6). A large amount of particular cases were studied, cf. e.g. [19] and references therein, yet this is a difficult mathematical problem with no generic formula. Nonetheless, some mathematical results characterizing intersections of sets hold with a fairly general level of validity and provide guidelines relevant for multivariate multifractal analysis. For notational simplicity, this section is restricted to $M = 2$, extensions to $M > 2$ are straightforward.

A first category of *generic* results are based on intuitions stemming from intersections of affine subspaces: e.g., in general, two planes in $\mathbb{R}^3$ intersect along a line, and more generally, in $\mathbb{R}^d$, affine subspaces intersect *generically* according to the *sum of codimensions rule*: $\dim(A \cap B) = \dim A + \dim B - d$, i.e. the "codimensions" $d - \dim A$ and $d - \dim B$ add up (this formula can yield a finite negative number, in which case, here and in the following, we use the convention that the corresponding set is empty). This result holds for numerous examples of fractal sets, in particular when the Hausdorff and Packing dimensions of one of the sets A or B coincide (as is typically the case for general Cantor sets); in that case "generically" has to be understood in the following sense: For a subset of positive measure among all rigid motions σ, $\dim(A \cap \sigma(B)) = \dim A + \dim B - d$. However the coincidence of Hausdorff and Packing dimensions is often not satisfied by the level sets $E(H)$. The only result that holds in all generality is the following: if A and B are two Borel subsets of $\mathbb{R}^d$, then, for a generic set of rigid motions σ, $\dim(A \cap \sigma(B)) \geq \dim A + \dim B - d$. This leads to a first guideline for multivariate multifractal spectra: When two recordings of experimental data are derived from unrelated experiments, then their singularity sets will be in generic position with respect to each other, and the genericity assumption will hold, yielding $D(H_1, H_2) \geq D(H_1) + D(H_2) - d$, whereas the stronger result

$$D(H_1, H_2) = D(H_1) + D(H_2) - d \tag{2.9}$$

will hold only for particular models.

For important classes of fractal sets, *sets with large intersection*, the codimension formula is not optimal as they satisfy $\dim(A \cap B) = \min(\dim A, \dim B)$; while such a formula may seem counterintuitive, fairly general frameworks where it holds were uncovered, cf. e.g., [20,21] and references therein. This is notably commonly met by *limsup sets*, obtained as follows: There exists a collection of sets A_n such that A is the set of points that belong to an infinite number of the A_n. This is particularly relevant for multivariate multifractal analysis as singularity sets $E^{\leq}(H)$ are of this type for several multifractal models, notably for additive stochastic processes, e.g. Lévy processes or random wavelet series, see [22,23] and ref. therein. For multivariate multifractal spectra, this leads to the alternative formula

$$D(H_1, H_2) = \min(D(H_1), D(H_2)) \tag{2.10}$$

which is expected to hold in competition with (2.9), at least for the sets $E^{\leq}(H)$, see Section 5(a)ii.

3. Multivariate extension of the multifractal formalism

(a) Minimizing sequences and compatibility

It is now well documented in the univariate setting that Hausdorff dimensions cannot be directly computed numerically. *Multifractal formalisms* are procedures allowing to *estimate* practically multifractal spectra from data. Additionally, they can also explain the shape of the structure functions by the shape of multifractal spectra (this actually was the motivation of the seminal article [5]).

Multifractal formalisms rely fundamentally on the definition of *multiscale quantities* d_λ. These quantities depend jointly on *time* x and *scale* 2^j and are defined as a nonnegative function $\lambda \to d_\lambda$ on dyadic cubes $\lambda (= \lambda(j,k)) \equiv \left[\frac{k_1}{2^j}, \frac{k_1+1}{2^j}\right) \times \cdots \times \left[\frac{k_d}{2^j}, \frac{k_d+1}{2^j}\right)$, with $j \in \mathbb{Z}$ and $k = (k_1, \cdots k_d) \in \mathbb{Z}^d$. We define the *log-leaders* of the *multiscale quantities* d_λ as

$$\ell_j(d_\lambda) = \frac{\log d_\lambda}{\log 2^{-j}}. \tag{3.1}$$

A key aspect of multiscale quantities in multifractal analysis is that they need to be tailored to the chosen local regularity index h, according to the following general framework.

Definition 1. *Let d_λ be a multiscale quantity. For $x \in \mathbb{R}^d$ let $\lambda_j(x)$ denote the dyadic cube of width 2^{-j} which contains x. A function $h(x)$ is called a pointwise exponent compatible with the multiscale quantity*

d_λ *if, for any x, there exists a sequence $\lambda_{j_n(x)}$ (with $j_n \to +\infty$) such that h(x) can be written as*

$$h(x) = \lim_{n \to +\infty} \ell_{j_n}\left(d_{\lambda_{j_n(x)}}\right). \tag{3.2}$$

The sequence $\lambda_{j_n(x)}$ is called a minimizing sequence for h at x. The couple formed by a multiscale quantity together with the associated compatible exponent is called a compatible couple.

Remarks: We use here the (standard) definition of pointwise exponents as functions that are defined at every point, where they take a unique value. However, other choices are possible. One can decide that $h(x)$ is only defined at the points x where the limit of $\ell_j(d_{\lambda_{j(x)}})$ when $j \to +\infty$ exists; this is the option taken to study multivariate multifractal analysis in [8,9]. On the opposite, one can consider *divergence points* where the limit does not exist. Obtaining information on the sets (such as their dimensions) is an important question which, in the context of multivariate analysis, has been addressed in [8,24,25]. One can also consider all possible limits of (3.2), in which case the exponent is not unique, but can be a subset of the real line, see [11] where this approach is followed. Numerous types of multiscale quantities (increments, oscillations, measures, wavelet coefficients,..., cf. e.g., [2] for reviews) were used to construct multifractal formalisms, mostly tied (sometimes incorrectly) to the choice of either the Hölder exponent or the local dimension as pointwise regularity index.

For functions, it is however now well documented that *wavelet leaders* are multiscale quantities associated with the Hölder exponent [1], and that wavelet p-leaders are associated with p-exponents [3,4]. These multiscale quantities are constructed from the coefficients of an orthonormal discrete wavelet transform (DWT) as follows. An orthonormal wavelet basis of $L^2(\mathbb{R}^d)$ can be defined from $2^d - 1$ compact support and regular enough functions $\psi^{(i)}$, referred to as mother-wavelets, as the collection of dilates and translates $2^{dj/2}\psi^{(i)}(2^j x - k)$, (for $j \in \mathbb{Z}$, and $k \in \mathbb{Z}^d$). The wavelet coefficients of the function $X(x)$ are $c_\lambda^{(i)} = 2^{dj} \int \psi^{(i)}(2^j x - k)X(x)dx$, and the corresponding *wavelet leaders* are

$$l_\lambda = \sup_{i,\lambda' \subset 3\lambda} |c_{\lambda'}^{(i)}|, \tag{3.3}$$

where 3λ denotes the union of λ with the $3^d - 1$ closest dyadic cubes of width 2^{-j}. Under weak global regularity assumptions, the Hölder exponent $h(x)$ is tied to wavelet leaders through

$$\forall x \in \mathbb{R}^d, \qquad h(x) = \liminf_{j \to +\infty} \ell_j(l_\lambda), \tag{3.4}$$

see [1], which clearly fits the general framework defined in (3.2). Similarly, p-exponents can also be derived from p-leaders by the same formula as (3.4), see [3,4].

For measures, the lower and upper local dimensions $\ell_\mu^-(x)$ and $\ell_\mu^+(x)$, can be obtained from the multiscale quantities $d_\lambda = \mu(3\lambda)$: $\ell_\mu^-(x) = \liminf_{j \to +\infty} \ell_j(d_{\lambda_{j(x)}})$ and $\ell_\mu^+(x) = \ell_j(d_{\lambda_{j(x)}})$, which also both fit in the general framework defined in (3.2).

(b) Multivariate multifractal formalism for synchronous exponents

(i) Synchronous exponents

The construction of multifractal formalisms in the multivariate setting requires the existence of minimizing sequences $\lambda_{j_n(x)}$ *shared by all exponents* associated with the different data components. This motivates the following definition.

Definition 2. *Let $(d_\lambda^k, h^k(x))$, $k = 1, \cdots, M$ be compatible couples. The $(d_\lambda^k, h^k(x))$ are synchronous if, for any x, there exists a sequence $\lambda_{j_n(x)}$ (with $j_n \to \infty$) which is a minimizing sequence for all $h^k(x)$.*

To illustrate this definition, let us discuss a few examples, with $M = 2$ for simplicity. If, for any x the sequence $\ell_j\left(d_{\lambda_{j(x)}}^1\right)$ has a limit when $j \to +\infty$, then, any subsequence is minimizing

for $h^1(x)$, so that, whatever the couple $(d_\lambda^2, h^2(x))$, it is synchronous with $(d_\lambda^1, h^1(x))$. This example corresponds e.g. to fractional Brownian motion, and to many functions or processes with continuous Hölder exponent. However, it does not correspond to classical multifractal models, for which $h(x)$ covers all its range when x takes values in any arbitrarily small interval.

If there exists an increasing function ω such that

$$\ell_j\left(d_{\lambda_{j(x)}}^2\right) = \omega\left(\ell_j\left(d_{\lambda_{j(x)}}^1\right)\right) + o(1) \quad \text{when } j \to +\infty$$

and if the two exponents are both computed by a $\liminf$ (or a $\limsup$), minimizing sequences for both exponents clearly are the same. Corresponding examples are discussed in Section 4. Importantly, this no longer holds if ω is decreasing, as we will see in Section 4. Additionally, the condition that d_λ^2 is an increasing function of d_λ^1 is not sufficient either to imply synchronicity.

(ii) Multivariate multifractal formalism and multivariate Legendre spectrum

A multifractal formalism relates multiscale quantities to the multifractal spectrum. The first one was originally proposed in the context of hydrodynamic turbulence and was constructed using increments as multiscale quantities [5]. Its multivariate extension was proposed several years later, again based on increments [6]. In hydrodynamic turbulence, this multivariate formalism is often called *grand canonical* in reference to thermodynamics, from where the seed intuitions and constructions of multifractal analysis stem, see [26].

This multivariate multifractal formalism is here reinterpreted in the general setting of synchronous exponents and compatible pairs of local regularity indices and multiscale quantities: $(d_\lambda^k, h^k(x))$, $k = 1, \cdots, M$. It is based on the *multivariate structure functions*

$$\forall r = (r_1, \cdots, r_M) \in \mathbb{R}^M, \qquad S(r, j) = 2^{-dj} \sum_{\lambda \in \Lambda_j} \left(d_\lambda^1\right)^{r_1} \cdots \left(d_\lambda^M\right)^{r_M}, \qquad (3.5)$$

where Λ_j denotes the collection of dyadic cubes of width 2^{-j}. Synchronicity constitutes a key requirement because $S(r, j)$ couples multiscale quantities $(d_\lambda^1, \cdots d_\lambda^M)$ at same scales and locations. Further, the *scaling function* is defined as

$$\zeta(r) = \liminf_{j \to +\infty} \frac{\log\left(S(r, j)\right)}{\log(2^{-j})}. \qquad (3.6)$$

The scaling function can be related to the multifractal spectrum as follows: if $x \in E(H)$, then the synchronicity of the $h_1(x), \cdots, h_M(x)$ together with (3.4) implies that there exist an infinite number of scales j such that for the same dyadic cubes,

$$d_{\lambda_j(x)}^1 \approx 2^{-H_1 j}, \cdots, d_{\lambda_j(x)}^M \approx 2^{-H_M j}.$$

Because $D(H)$ is the *fractal* dimension of $E(H)$, the number of cubes of size 2^{-j} required to cover $E(H)$ is $\sim 2^{jD(H)}$. Therefore $S(r, j)$ can also be rewritten as $S(r, j) \simeq \sum_h 2^{-dj} 2^{jD(H)} 2^{-(H_1 r_1 + \cdots + H_M r_M)j}$. When $j \to +\infty$, the dominant contribution stems from the smallest exponent; indeed, the other contributions are exponentially smaller as a function of j and will ultimately be negligible in the limit $j \to +\infty$, thus yielding

$$\zeta(r) = \inf_{H \in \mathbb{R}^M}(d - D(H) + H \cdot r), \quad \text{where } H \cdot r = H_1 r_1 + \cdots + H_M r_M. \qquad (3.7)$$

This leads to define the *multivariate Legendre spectrum* as the M-variable Legendre transform of the multivariate scaling function:

$$\forall H \in \mathbb{R}^M, \qquad L(H) = \inf_{r \in \mathbb{R}^M}(d - \zeta(r) + H \cdot r). \qquad (3.8)$$

General properties of $L(H)$ (without assuming synchronicity) are proved in [13,14]. Important results of [14,15] (and refs. therein) state that the multifractal formalism is satisfied for couples of *generic* functions (both in the sense of Baire and prevalence) in given Besov or oscillation spaces.

(c) Upper bound: multivariate multifractal and Legendre spectra

In a univariate setting, i.e. $M = 1$, under weak global regularity assumptions, the Legendre spectrum systematically yields an upper bound for the multifractal spectrum: $L(H) \geq D(H)$ [1]. Theorem 1 establishes that this inequality extends to a multivariate setting in the synchronous case (the informal derivation sketched above does not constitute a mathematical proof).

Theorem 1. *Let $(d_\lambda^k, h^k(x))$, $k = 1, \cdots, M$, denote a collection of compatible couples which are synchronous. The multivariate Legendre and multifractal spectra satisfy:*

$$\forall H \in \mathbb{R}^M, \qquad D(H) \leq L(H). \tag{3.9}$$

Additionally, the spectra $D^{\leq}$ and $D^{\geq}$ satisfy

$$D^{\leq}(H) \leq \inf_{r \in (\mathbb{R}^+)^M} (d - \zeta(r) + H \cdot r), \text{ and } D^{\geq}(H) \leq \inf_{r \in (\mathbb{R}^-)^M} (d - \zeta(r) + H \cdot r). \tag{3.10}$$

Remark: Inequalities (3.10) bound $D^{\leq}$ (resp. $D^{\geq}$) by functions that are increasing (resp. decreasing) in all variables. In practice, for concave spectra, it yields a bound for the part of the spectrum that is increasing (resp. decreasing) in all variables $H_1, \ldots H_m$.

Proof: Let $H = (H_1, \ldots, H_M)$ be fixed, and let $\varepsilon > 0$. For $j \geq 0$, we denote by $F(H, j, \varepsilon)$ the set of dyadic cubes of width 2^{-j} defined by the conditions

$$2^{(-H_1 - \varepsilon)j} \leq d_{\lambda_1} \leq 2^{(-H_1 + \varepsilon)j}, \ldots, 2^{(-H_M - \varepsilon)j} \leq d_{\lambda_M} \leq 2^{(-H_M + \varepsilon)j}; \tag{3.11}$$

we denote by $N(H, j, \varepsilon)$ the cardinality of this set. By restricting the sum in (3.5) to the elements of $F(H, j, \varepsilon)$, and using (3.11) it follows that

$$\forall r \in \mathbb{R}^M, \qquad 2^{-dj} N(H, j, \varepsilon) 2^{-(r_1 H_1 + \varepsilon|r_1|)j} \ldots 2^{-(r_M H_M + \varepsilon|r_M|)j} \leq S(r_1, \ldots r_M, j);$$

and from (3.6) we obtain that, for j large enough, $S(r, j) \leq 2^{-j(\zeta(r) - \varepsilon)}$; thus

$$N(H, j, \varepsilon) \leq 2^{j(d - \zeta(r) + \varepsilon + r_1 H_1 + \varepsilon|r_1| + \cdots + r_M H_M + \varepsilon|r_M|)}. \tag{3.12}$$

It follows from (3.4) and the synchronicity hypothesis that

$$\text{if } x \in E(H), \text{ then} \qquad \forall \varepsilon > 0, \quad x \in \limsup_{j \to +\infty} F(H, j, \varepsilon).$$

Thus,

$$\forall J > 0, \qquad E(H) \subset \bigcup_{j \geq J} F(H, j, \varepsilon).$$

Let $A = d - \zeta(r) + \varepsilon + r_1 H_1 + \varepsilon|r_1| + \cdots + r_M H_M + \varepsilon|r_M|$; because of (3.12), $F(H, j, \varepsilon)$ is composed of at most 2^{Aj} dyadic cubes of width 2^{-j}. Using these cubes as 2^{-j}-covering of $E(H)$, (3.12) yields

$$\sum_{j \geq J} \sum_{\lambda \in F(H, j, \varepsilon)} (diam(\lambda))^\delta \leq \sum_{j \geq J} 2^{Aj} (2^{-j})^\delta$$

which is finite as soon as $\delta > A$. It follows that the Hausdorff dimension of $E(H)$ is bounded by A. Since this is true $\forall \varepsilon > 0$, we obtain that $D(H)$ is bounded by $d - \zeta(r) + r_1 H_1 + \cdots + r_M H_M$. Since this holds for any $r \in \mathbb{R}^M$, the first statement of the theorem is proved. The proofs of the other two statements are similar.

Remarks: A similar argument is used by M. Ben Slimane in [14] in order to derive the multivariate multifractal spectra of generic functions in a product of function space. Additionally, in the setting of selfsimilar measures satisfying the Open Set Condition, L. Olsen introduced a related quantity [11]: x being fixed, he considers the sets $A(x)$ of exponents $(H_1, \cdots H_M)$ which

are accumulation points of subsequences of the multivariate quantities

$$\left(\ell_j(d^1_{\lambda_j(x)}), \cdots, \ell_j(d^M_{\lambda_j(x)}) \right).$$

Then, for any fixed set $C \subset \mathbb{R}^M$, he derives the Hausdorff dimension of the set of points x for which $A(x) \subset C$.

For a given multiscale quantity (d_λ), several exponents can be associated through Definition 1, each leading to a different definition of $E(H)$. However, some subsets, which only depend on the multiscale quantity (and not on the way that the subsequence is picked in (3.2)) play an important role in theoretical multifractal analysis: the *regular points* defined as the points where log-leaders have a limit when $j \to +\infty$, i.e. when the limit in (3.2) is the same for any subsequence. We define the corresponding sets as

$$\forall H = (H_1, \dots H_M), \qquad E_{Reg}(H) = \left\{ x: \quad \forall k = 1, \dots M, \quad \ell_j \left(d^k_{\lambda_{j(x)}} \right) \to_{j \to +\infty} H_k \right\}. \quad (3.13)$$

By construction, the exponents h_k are synchronous at these points, so that Theorem 1 applies, and

$$\forall H \in \mathbb{R}^M, \qquad \dim(E_{Reg}(H)) \le L(H). \quad (3.14)$$

Clearly $E_{Reg}(H) \subset E(H)$; in some situations, the information supplied by their dimension is poor; e.g., in the counterexample worked out in Section 5(a)i, all sets $E_{Reg}(H)$ are empty. On the other hand, they can also be "large", i.e. have the same Hausdorff dimension as $E(H)$: it is the case e.g. for *univariate binomial cascades* (see Section 4(c)ii). Regular points are considered in [9], in particular in order to perform the multivariate analysis of couples of selfsimilar measures satisfying Hutchinson's separation condition.

4. Deterministic bivariate dyadic binomial cascades

Univariate multiplicative cascades, consisting of measures supported by $[0, 1]$ and obtained from a recursive construction, constitute archetypal multifractal constructions [27]. It is thus natural to consider multivariate extensions and to investigate the multivariate multifractal spectrum, formalism and Legendre spectrum. In this section we consider the example of bivariate cascades supplied by binomial cascades.

Note that the bivariate (and even multivariate) spectra of large classes of measures (including binomial cascades) have extensively been studied, and many key results have already been obtained. For instance, L. Olsen in [9,11] considered selfsimilar and multiplicative measures associated with an IFS satisfying the Open Set Condition, and the dimension of sets of divergence points (i.e. points x at which the limit of mutivariate log-leaders -following our terminology- does not exist) have been calculated for such measures. The multifractal analysis of Gibbs measures associated with continuous potentials invariant under smooth dynamical systems was performed, e.g. in [8], and it has been shown that the support of the multifractal spectrum can be nonconvex. Our approach is quite different, and complementary, to theirs. First, these authors mainly focus on local exponents (that can be Birkhoff averages, local entropies, or Lyapunov exponents) defined as limits, while we always work with liminf exponents (see formulas (3.4) and (2.2)). Many (surprising) behaviors are not observed when restricting the study to limits, as will be illustrated in this section and the next. Second, in the above references, the Hausdorff dimension of divergence points is computed, but the question of the dimension of the level sets associated with these divergence points is not addressed as directly as in the present paper. Third, the validity of the multifractal formalism is tackled only through the prism of limit exponents, whereas the use of exponents defined by liminfs reveals some new remarkable phenomena (which led us to study in details variations of the multifractal formalism, see Section 5(b) for instance). Indeed, if one disregards the points at which the limits do not exist, the phenomenon described below cannot be put into light (Theorem 3, with very different shapes for the scaling functions and the L^q-spectra of a bivariate binomial cascade according to the choice of the parameters of the cascades); and indeed, it has never been observed before. In particular, the fact that the Legendre

transform of the L^q-spectrum (which serves as upper bound for the multifractal spectrum in all the references above) lies below the multifractal spectrum of the bivariate cascade, was clearly not detected previously.

The exponent considered in this section is the lower local dimension, see Section 2(a). To simplify computations we drop the 2^{-j} in the definition of structure functions and, accordingly, Legendre transforms are defined by $L(H) = \inf_r(r \cdot H - \zeta(r))$.

(a) Univariate cascades

Dyadic intervals are indexed by "dyadic words" (i.e. finite sequences) with "letters" $\varepsilon_i \in \{0, 1\}$: If $j \geq 1$, $\Sigma_j = \{0, 1\}^j$ denotes the set of words of length j with letters $\in \{0, 1\}$. A word $w \in \Sigma_j$ of length $|w| = j$ is written $w = \varepsilon_1 \varepsilon_2 \cdots \varepsilon_j$. The corresponding dyadic interval λ_w of generation j is

$$\lambda_w = [x_w, x_w + 2^{-j}), \quad \text{where } x_w \text{ is the real number } x_w = \sum_{k=1}^{\infty} \varepsilon_k 2^{-k}. \tag{4.1}$$

This defines a mapping between Σ and $[0, 1]$ (which is not one to one, since dyadic points are encoded by two different words). If w is a (possibly infinite) word longer than j, we define

$$N_j^0(w) = \#\{\varepsilon_i : 1 \leq i \leq j \text{ and } \varepsilon_i = 0\} \in \{0, 1, ..., j\},$$

i.e. $N_j^0(w)$ is the number of 0s among the first j digits of w.

Let $p \in [0, 1]$. The binomial measure μ_p is the probability measure supported by $[0, 1]$ and constructed iteratively as follows: $\mu_p([0, 1]) = 1$; if λ_w is a dyadic interval, since λ_{w0} and λ_{w1} are respectively the left and right half of λ_w, then $\mu_p(\lambda_{w0}) = p\mu_p(\lambda_w)$ and $\mu_p(\lambda_{w1}) = (1 - p)\mu_p(\lambda_w)$; μ_p is thus defined on all dyadic intervals and extends to Borel sets of $[0, 1]$. If w has length j, then

$$\mu_p(\lambda_w) = p^{N_j^0(w)}(1 - p)^{j - N_j^0(w)}. \tag{4.2}$$

Note that $\mu_{1/2}$ is the Lebesgue measure, and μ_0 and μ_1 are the Dirac masses at 1 and 0, respectively. The scaling function of μ_p is $\eta_{\mu_p}(r) = -\log_2(p^r + (1 - p)^r)$, and μ_p verifies the multifractal formalism: $D_{\mu_p}(H) = \inf_{r \in \mathbb{R}}(rH - \eta_{\mu_p}(r))$.

(b) Bivariate multifractral spectrum

We introduce the exponents

$$H_{p,\min} = -\log_2(1 - p), \quad H_{p,m} = (-\log_2(p) - \log_2(1 - p))/2, \quad H_{p,\max} = -\log_2(p). \tag{4.3}$$

When $p < 1/2$, $H_{p,\min} < H_{p,m} < H_{p,\max}$, while the order is reversed when $p > 1/2$. We use the exponents $H_{p,\min}, H_{q,\min}, ...$, with two parameter values p and q. We study the joint spectrum of two binomial measures (μ_p, μ_q) when $p, q < 1/2$ and $p < 1/2 < q$. These two situations yield very different spectra: Intuitively, the two cascades are correlated when $p, q < 1/2$ and anti-correlated when $p < 1/2 < q$ (cf. Figs. 1 and 2). Let us introduce the affine function

$$G_{p,q}(x) = \rho_{p,q}(x + \log_2(1 - p)) - \log_2(1 - q), \quad \text{where } \rho_{p,q} = \frac{\log_2 q - \log_2(1 - q)}{\log_2 p - \log_2(1 - p)}. \tag{4.4}$$

$G_{p,q}$ has positive slope when $p, q < 1/2$, and negative slope when $p < 1/2 < q$. The following result of [13] yields the bivariate multifractal spectrum of the couple (μ_p, μ_q).

Theorem 2. *Let $p, q \in (0, 1)$, and let μ_p and μ_q be two binomial measures on $[0, 1]$.*

(a) *If $0 < p, q < 1/2$, the joint spectrum $D_{(\mu_p, \mu_q)}$ of (μ_p, μ_q) is supported by the segment $\{(H, G_{p,q}(H)) : H \in [H_{p,\min}, H_{p,\max}]\}$ where*

$$D_{(\mu_p, \mu_q)}(H, G_{p,q}(H)) = D_{\mu_p}(H) \,(= D_{\mu_q}(G_{p,q}(H)). \tag{4.5}$$

(b) *If $0 < p < 1/2 < q < 1$, then the joint spectrum $D_{(\mu_p, \mu_q)}$ is supported by the triangle*
$$\mathcal{T} = \Big\{ (H, H') : H \in [H_{p,\min}, H_{p,\max}] \text{ and } H' \in [H_{q,\min}, G_{p,q}(H)] \Big\} \text{ where}$$

$$\forall (H, H') \in \mathcal{T} \qquad D_{(\mu_p, \mu_q)}(H, H') = \min(D_{\mu_p}(H), D_{\mu_q}(H')).$$

(c) Bivariate multifractal formalism and Legendre spectrum

In this section we determine the Legendre spectrum of bivariate binomial cascades. For that purpose, we calculate the scaling function $\zeta_{p,q}$ (3.6) based on the structure functions $S((r_1, r_2), j)$. As a first step, we compute the following simpler "one box" scaling function $\eta_{p,q}$, where the multiscale quantity considered is $\mu(\lambda)$ instead of the usual $\mu(3\lambda)$

$$\eta_{p,q}(r_1, r_2) = \liminf_{j \to +\infty} \frac{1}{-j} \log_2 T((r_1, r_2), j), \quad \text{where } T((r_1, r_2), j) = \sum_{w \in \Sigma_j} \mu_p(\lambda_w)^{r_1} \mu_q(\lambda_w)^{r_2}$$

and its Legendre transform $L_{p,q}(H_1, H_2) = \inf_{r_1, r_2}(r_1 H_1 + r_2 H_2 - \eta_{p,q}(r_1, r_2))$.

Proposition 4.1. *The "one box" scaling function of (μ_p, μ_q) is $\eta_{p,q}(r_1, r_2) = -\log_2(p^{r_1} q^{r_2} + (1-p)^{r_1}(1-q)^{r_2})$ and*

$$L_{p,q}(H_1, H_2) = \begin{cases} D_{\mu_p}(H_1) & \text{when } H_1 \in [H_{p,\min}, H_{p,\max}] \text{ and } H_2 = G_{p,q}(H_1) \\ -\infty & \text{otherwise.} \end{cases} \tag{4.6}$$

Proof. An immediate computation shows that

$$T((r_1, r_2), j) = \sum_{w \in \Sigma_j} (p^{r_1} q^{r_2})^{N_j^0(w)} ((1-p)^{r_1}(1-q)^{r_2})^{j - N_j^0(w)}$$

$$= \sum_{k=0}^{j} \binom{j}{k} (p^{r_1} q^{r_2})^k ((1-p)^{r_1}(1-q)^{r_2})^{j-k} = (p^{r_1} q^{r_2} + (1-p)^{r_1}(1-q)^{r_2})^j,$$

so that $\eta_{p,q}(r_1, r_2) = -\log_2(p^{r_1} q^{r_2} + (1-p)^{r_1}(1-q)^{r_2})$.

Moving to the 2-dimensional Legendre transform of $\eta_{p,q}$, we compute the partial derivatives

$$\frac{\partial \eta_{p,q}}{\partial r_1}(r_1, r_2) = \frac{-p^{r_1} q^{r_2} \log_2(p) - (1-p)^{r_1}(1-q)^{r_2} \log_2(1-p)}{p^{r_1} q^{r_2} + (1-p)^{r_1}(1-q)^{r_2}}$$

$$\text{and} \quad \frac{\partial \eta_{p,q}}{\partial r_2}(r_1, r_2) = \frac{-p^{r_1} q^{r_2} \log_2(q) - (1-p)^{r_1}(1-q)^{r_2} \log_2(1-q)}{p^{r_1} q^{r_2} + (1-p)^{r_1}(1-q)^{r_2}}.$$

Note that $\frac{\partial \eta_{p,q}}{\partial r_2}(r_1, r_2) = G_{p,q}\Big(\frac{\partial \eta_{p,q}}{\partial r_1}(r_1, r_2) \Big)$. This affine relationship shows that the Legendre spectrum $L_{p,q}$ of (μ_p, μ_q) (based on the scaling function $\eta_{p,q}$) is supported by the straight line $(H_1, G_{p,q}(H_1))$. This yields (4.6). $\square$

We call $\zeta_{p,q}$ the scaling function associated with (μ_p, μ_q), and $L_{(\mu_p, \mu_q)}$ its Legendre transform.

When $0 < p < 1/2 < q < 1$, we introduce the following notations: for $(H_1, H_2) \in \mathcal{T}$, we call $(\widetilde{H_1}, H_{q,\max})$ (resp. $(H_{p,\min}, \widetilde{H_2})$) the intersection points of the straight line passing through (H_1, H_2) and slope $\rho_{p,q}$ (recall (4.4)) with the line $\{(H, H') : H' = H_{q,\max}\}$ (resp. with the line $(\{(H, H') : H = H_{p,\min}\})$. Namely, $\widetilde{H_1} = H_1 + \frac{H_{q,\max} - H2}{\rho_{p,q}}$ and $\widetilde{H_2} = H_2 + \rho_{p,q}(H_1 - \widetilde{H_1})$.

Theorem 3. *Let $p, q \in (0, 1)$, and let μ_p and μ_q be two binomial measures on $[0, 1]$.*

(a) *If $0 < p, q < 1/2$, the couples $(\mu_p(3\lambda), \ell_{\mu_p}^-)$ and $(\mu_q(3\lambda), \ell_{\mu_q}^-)$ are synchronous and the couple (μ_p, μ_q) satisfies the multifractal formalism: $\forall H, L_{p,q}(H) = L_{(\mu_p, \mu_q)}(H) = D_{(\mu_p, \mu_q)}(H)$.*

(b) *If $0 < p < 1/2 < q < 1$, the couples $(\mu_p(3\lambda), \ell_{\mu_p}^-)$ and $(\mu_q(3\lambda), \ell_{\mu_q}^-)$ are not synchronous, and the multifractal spectrum is not bounded by the Legendre spectrum. More precisely, lhe joint*

scaling function $\zeta_{p,q}(r_1, r_2)$ of (μ_p, μ_q) is given by:

$$\zeta_{p,q}(r_1, r_2) = \begin{cases} -r_1 \log_2(1-p) - r_2 \log_2(q) & \text{if } \left(\frac{p}{1-p}\right)^{r_1} + \left(\frac{1-q}{q}\right)^{r_2} \leq 1 \\ \eta_{p,q}(r_1, r_2) & \text{otherwise} . \end{cases} \quad (4.7)$$

The corresponding Legendre transform $L_{(\mu_p, \mu_q)}$ is the following: for (H_1, H_2), set $r = \frac{\widetilde{H_1} - H_{\min,p}}{H_{\max,p} - H_{\min,p}}$ and $r' = \frac{\|(H_1, H_2) - (\widetilde{H_1}, H_{\max,q})\|}{\|(\widetilde{H_2}, H_{\min,p}) - (\widetilde{H_1}, H_{\max,q})\|}$. Then for every $(H_1, H_2) \in \mathcal{T}$,

$$L_{(\mu_p, \mu_q)}(H) = r \times D_{\mu_p}\Big(H_{\max,p} + r' \cdot (H_{\min,p} - H_{\max,p})\Big). \quad (4.8)$$

The map $L_{(\mu_p, \mu_q)}$, though based on unpleasant formulas, is simply interpreted in geometric terms: it is the surface on $\mathcal{T}$ defined as the semi-cone with extremity $(-\log_2(1-p), -\log_2(q))$ and with border the Legendre transform $L_{p,q}$ of $\eta_{p,q}$.

Theorem 3 illustrates the necessity of the synchronicity requirement for the upper bound given by Theorem 1. Figures 1 and 2 illustrate Theorem 3, showing the corresponding theoretical Legendre spectra and their numerical estimations. The proof of this theorem is detailed in the next subsections.

(i) The case $0 < p, q < 1/2$

We check that, when p, q are both less than $1/2$, the two cascades are synchronous. First, note that, for any measure ν, $\nu(3\lambda)$ can be replaced (up to a factor 3) by the maximum of $\nu(\lambda)$, $\nu(\lambda - 2^{-j})$ and $\nu(\lambda + 2^{-j})$. We will prove that this maximum is reached at the same interval for the two measures μ_p and μ_q. Indeed, if λ_w denotes this interval of largest measure, then (4.2) implies that

$$\mu_p(\lambda_w) = p^{N_j^0(w)}(1-p)^{j-N_j^0(w)} \quad \text{and} \quad \mu_q(\lambda_w) = q^{N_j^0(w)}(1-q)^{j-N_j^0(w)}$$

from which it follows that the corresponding log-leaders are related by an affine relationship

$$\log_2(\mu_q(\lambda_w)) = \rho_{p,q} \log_2(\mu_p(\lambda_w)) + j\theta_{p,q} \quad \text{where } \theta_{p,q} = \log_2(1-q) - \rho_{p,q} \log_2(1-p).$$

Since $\rho_{p,q}$ is positive when p and q are on the same side of $1/2$, this implies synchronicity.

We now check that the joint scaling function of (μ_p, μ_q) is $\zeta_{p,q}(r_1, r_2) = \eta_{p,q}(r_1, r_2)$. Let $w \in \Sigma_j$ and λ_w. Clearly, $\mu_p(3\lambda_w) = \mu_p(\lambda_w - 2^{-j}) + \mu_p(\lambda_w) + \mu_p(\lambda_w + 2^{-j})$. Denote by λ the interval with the largest μ_p-mass in these three terms; then $\mu_p(\lambda) \leq \mu_p(3\lambda_w) \leq 3\mu_p(\lambda)$. As noticed before, the same interval has the largest mass for μ_p and μ_q, and $\mu_q(\lambda) \leq \mu_q(3\lambda_w) \leq 3\mu_q(\lambda)$. As a conclusion, $\mu_p(3\lambda_w)^{r_1}\mu_q(3\lambda_w)^{r_2} \sim \mu_p(\lambda)^{r_1}\mu_q(\lambda)^{r_2}$ for one $\lambda \in \{\lambda_w - 2^{-j}, \lambda_w, \lambda_w + 2^{-j}\}$; thus, if $r_1, r_2 > 0$, then

$$S((r_1, r_2), j) = \sum_{w \in \Sigma_j} \mu_p(3\lambda_w)^{r_1}\mu_q(3\lambda_w)^{r_2} \leq C \sum_{w \in \Sigma_j} \mu_p(\lambda_w)^{r_1}\mu_q(\lambda_w)^{r_2} = CT((r_1, r_2), j).$$

Let us now focus on one product $\mu_p(\lambda_w)^{r_1}\mu_q(\lambda_w)^{r_2}$ for a given word $w \in \Sigma_j$. Considering the word $w' = w01 \in \Sigma_{j+2}$, we remark that $p^{-2}\mu_p(\lambda_w) \leq \mu_p(3\lambda_{w'}) \leq \mu_p(\lambda_w)$, and similarly $q^{-2}\mu_q(\lambda_w) \leq \mu_q(3\lambda_{w'}) \leq \mu_q(\lambda_w)$. Hence,

$$C\mu_p(3\lambda_{w'})^{r_1}\mu_q(3\lambda_{w'})^{r_2} \leq \mu_p(\lambda_w)^{r_1}\mu_q(\lambda_w)^{r_2} \leq C'\mu_p(3\lambda_{w'})^{r_1}\mu_q(3\lambda_{w'})^{r_2},$$

for two constants $C, C' > 0$ that depend only on p, q, r_1 and r_2. In particular,

$$T((r_1, r_2), j) := \sum_{w \in \Sigma_j} \mu_p(\lambda_w)^{r_1}\mu_q(\lambda_w)^{r_2} \leq C'' \sum_{w' \in \Sigma_{j+2}} \mu_p(3\lambda_{w'})^{r_1}\mu_q(3\lambda_{w'})^{r_2} = S((r_1, r_2), j+2).$$

Thus $S((r_1, r_2), j) \leq T((r_1, r_2), j) \leq C''S((r_1, r_2), j+2)$, so that $\eta_{p,q}(r_1, r_2) = \zeta_{p,q}(r_1, r_2)$. The argument is the same if r_1 or r_2 are negative, exchanging upper and lower bounds.

Keeping Theorem 2 in mind, this proves that the bivariate multifractal formalism holds for the pair (μ_p, μ_q) in that case. The situation is illustrated numerically in Fig. 1, where it is shown that
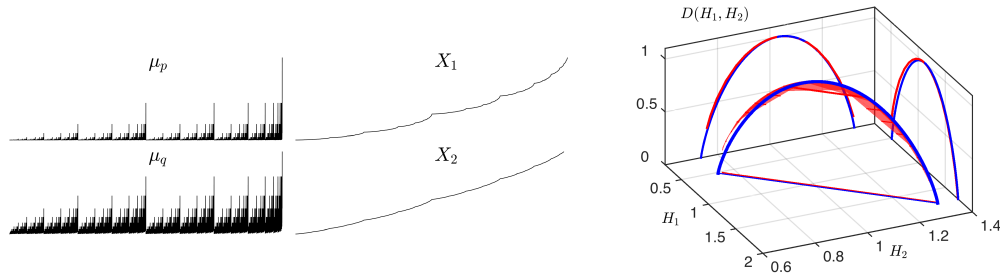
Figure 1. Multifractal analysis of bivariate binomial cascades if $p, q < 1/2$. Left: The measures (μ_p, μ_q) and their cumulative density functions ($M = 2$). Right: theoretical bivariate multifractal spectrum $D(H)$ (blue), estimated Legendre spectrum $L(H)$ (red surface) and the corresponding marginal spectra (red and blue curves in the H_1 and H_2 planes). In this case, the support of the multivariate multifractal spectrum $D(H)$ collapses to a line in the (H_1, H_2) plane. The numerically estimated Legendre spectrum is found to tightly follow $D(H)$, in agreement with the fact that the synchronicity assumption is satisfied and the multifractal formalism holds.

the numerical estimate for $L(H)$ is in excellent agreement with the theoretically predicted shape, and therefore with the bivariate multifractal spectrum $D(H)$.

(ii) The case $0 < p < 1/2 < q$

Let $w \in \Sigma_j$ be a word ending with a 0; denote by $w' \in \Sigma_j$ the binary word such that $x_w = x_w - 2^{-j}$, so that w' ends with a 1. Obviously, $\mu_p(3\lambda_w) = \mu_p(\lambda_{w'}) + \mu_p(\lambda_w) + \mu_p(\lambda_w + 2^{-j})$ and $\mu_p(3\lambda_{w'}) = \mu_p(\lambda_{w'} - 2^{-j}) + \mu_p(\lambda_{w'}) + \mu_p(\lambda_w)$. Since the last letter of w' is 1, $\mu_p(\lambda_{w'} - 2^{-j}) = \frac{p}{1-p}\mu_p(\lambda_{w'})$, and similarly $\mu_p(\lambda_w) = \frac{p}{1-p}\mu_p(\lambda_w + 2^{-j})$. We conclude that $\mu_p(3\lambda_w)$ and $\mu_p(3\lambda_w - 2^{-j})$ have the same order of magnitude: The ratio $\mu_p(3\lambda_w)/\mu_p(3\lambda_{w'})$ is bounded above and below by constants depending only on p. The same holds for $\mu_q(3\lambda_w)/\mu_q(3\lambda_{w'})$. It follows that $\mu_p(3\lambda_w)^{r_1}\mu_q(3\lambda_w)^{r_2}$ and $\mu_p(3\lambda_{w'})^{r_1}\mu_q(3\lambda_{w'})^{r_2}$ have the same order of magnitude.

Subsequently, in the sum (3.5) defining $S((r_1, r_2), j)$, it is sufficient to study the terms corresponding to words w ending with a 1. Notice that Σ_j can be encoded as

$$\Sigma_j = \{1^{(j)}\} \cup \bigcup_{\ell=0}^{j-1} \bigcup_{w \in \Sigma_\ell} \{w \cdot 0 \cdot 1^{(j-\ell-1)}\},$$

where $1^{(\ell)}$ (resp. $0^{(\ell)}$) stands for the word of length ℓ containing only 1s (resp. 0s), and Σ_0 contains only the empty word. In this decomposition, words ending with a 1 correspond to $\ell = 0, ..., j - 2$. The discussion above tells us that it remains to study the asymptotic behavior of

$$S((r_1, r_2), j) \sim \sum_{\ell=0}^{j-2} \sum_{w \in \Sigma_\ell} \mu_p(3\lambda_{w \cdot 0 \cdot 1^{(j-\ell-1)}})^{r_1} \mu_q(3\lambda_{w \cdot 0 \cdot 1^{(j-\ell-1)}})^{r_2}.$$

If a word $w' \in \Sigma_j$ is written as $w' = w \cdot 0 \cdot 1^{(j-\ell-1)}$ for some $w \in \Sigma_\ell$, then the dyadic point $x_{w''} = x_{w'} + 2^{-j}$ (recall (4.1)) is associated with the binary word $w'' = w \cdot 1 \cdot 0^{(j-\ell-1)}$. So, $\mu_p(3\lambda_{w'}) = \mu_p(\lambda_{w \cdot 0 \cdot 1^{(j-\ell-1)}}) + \mu_p(\lambda_{w \cdot 0 \cdot 1^{(j-\ell-1)}}) + \mu_p(\lambda_{w''})$ with

$$\mu_p(\lambda_{w''}) = \mu_p(\lambda_{w \cdot 0 \cdot 1^{(j-\ell-1)}}) \left(\frac{p}{1-p}\right)^{j-1-\ell}. \tag{4.9}$$

the same being true for μ_q (with q replacing p).

The relative positions of p and q imply that the word λ for which the maximum is reached in (4.9) is not the same for μ_p and for μ_q. Indeed, in (4.9), the first two terms are equivalent, and the third one is smaller since $p < 1/2 < 1 - p$. On the opposite, when considering (4.9) for μ_q, the first two terms are equivalent, but the third one is the largest since $q > 1/2 > 1 - q$. Consequently,
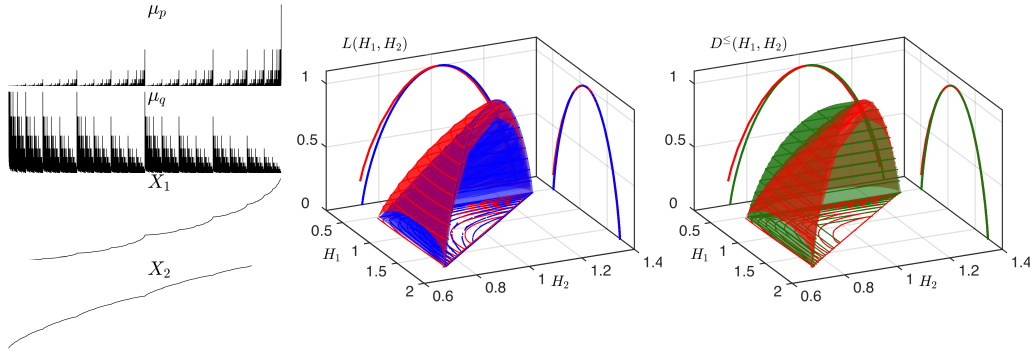
Figure 2. Multifractal analysis of bivariate cascades for the case $p < 1/2 < q$. Left: The measures (μ_p, μ_q) and their cumulative density functions ($M = 2$). Superposition of the theoretical (blue) and estimated (red) Legendre spectra $L(H)$ (center) and of the theoretical bivariate multifractal spectrum $D(H)$ (green) and the estimated Legendre spectrum $L(H)$ (red) (right); the corresponding marginal spectra are plotted in the H_1 and H_2 planes. The numerical estimate of the Legendre spectrum $L(H)$ (in red) is in excellent agreement with the theoretical prediction (in blue) but, as a consequence of the failure of synchronicity, it does not give an upper bound for the multifractal spectrum $D(H)$ (in green), and the multifractal formalism does not hold.

$\mu_p(3\lambda_{w'}) \sim \mu_p(\lambda_w)p(1-p)^{j-\ell-1}$ and $\mu_q(3\lambda_{w'}) \sim \mu_q(\lambda_w)(1-q)q^{j-\ell-1}$. We can now estimate

$$S((r_1, r_2), j) \sim \sum_{\ell=0}^{j-2} \sum_{w \in \Sigma_\ell} \mu_p(\lambda_{w01^{(j-\ell-1)}})^{r_1} \mu_q(\lambda_{w \cdot 1 \cdot 0^{(j-\ell-1)}})^{r_2}$$

$$\sim \sum_{\ell=0}^{j-2} \sum_{w \in \Sigma_\ell} \mu_p(\lambda_w)^{r_1} p^{r_1}(1-p)^{r_1(j-\ell-1)} \mu_q(\lambda_w)^{r_2}(1-q)^{r_2} q^{r_2(j-\ell-1)}$$

$$= p^{r_1}(1-q)^{r_2}(1-p)^{r_1(j-1)} q^{r_2(j-1)} \sum_{\ell=0}^{j-1} ((1-p)^{-r_1} q^{-r_2})^\ell \sum_{w \in \Sigma_\ell} \mu_p(\lambda_w)^{r_1} \mu_q(\lambda_w)^{r_2}$$

$$= p^{r_1}(1-q)^{r_2}(1-p)^{r_1(j-1)} q^{r_2(j-1)} \sum_{\ell=0}^{j-1} ((1-p)^{-r_1} q^{-r_2})^\ell (p^{r_1} q^{r_2} + (1-p)^{r_1}(1-q)^{r_2})^j$$

$$= p^{r_1}(1-q)^{r_2}(1-p)^{r_1(j-1)} q^{r_2(j-1)} \sum_{\ell=0}^{j-1} \left(\left(\frac{p}{1-p} \right)^{r_1} + \left(\frac{1-q}{q} \right)^{r_2} \right)^j .$$

The sum above behaves differently according to whether $\left(\frac{p}{1-p} \right)^{r_1} + \left(\frac{1-q}{q} \right)^{r_2} \leq 1$ or > 1, hence there is a phase transition in the values of $\zeta_{p,q}$. A quick computation yields (4.7).

The Legendre transform of the scaling function $-r_1 \log_2(1-p) - r_2 \log_2(q)$ is the Dirac mass (with value 0) at $(H_1, H_2) = (-\log_2(1-p), -\log_2(q))$, and $-\infty$ otherwise. Thus, the Legendre transform $L_{(\mu_p,\mu_q)}$ of $\zeta_{p,q}$ is the surface in $\mathbb{R}^3$ defined by the semi-cone with extremity $(-\log_2(1-p), -\log_2(q))$ and with border the Legendre transform of $\eta_{p,q}$. The formula (4.8) is simply the analytic formula corresponding to this semi-cone.

The verification that the multifractal formalism does not give an upper bound of the multifractal spectrum is now straightforward and, as a consequence, it follows that (in contradistinction with the case $0 < p, q < 1/2$), the two couples $(\mu_p(3\lambda), \ell_{\bar{\mu}_p})$ and $(\mu_q(3\lambda), \ell_{\bar{\mu}_q})$ are not synchronous if p and q are not on the same side of $1/2$ (otherwise Theorem 1 would imply that the upper bound holds). An illustration is provided in Fig. 2, which plots the theoretical multifractal spectrum $D(H)$, the theoretical Legendre spectrum $L_{(\mu_p,\mu_q)}(H)$ and its a numerical estimate. Clearly, both the theoretical and the numerically estimated function $L_{(\mu_p,\mu_q)}(H)$ are smaller than $D(H)$ and hence do not provide an upper bound for $D(H)$. This motivates a careful

study of the validity of the multifractal formalism when synchronicity fails. In the next section we will see other occurrences of this phenomenon.

   Remark: For both univariate cascades, the regular points (see (3.13)) are exactly the points where $N_J^0(\omega)/j$ has a limit. The dimensions of these sets are the same as for those where the limit is a $\liminf$. It follows that, for each cascade $\dim(E_{Reg}(H)) = D_{\mu_p}(H)$, and the bivariate spectrum associated with regular points is given by (4.5) in both cases. Therefore, the bivariate spectrum associated with regular points satisfies the upper bound (3.14) (even when p and q are not on the same side of $1/2$).

5. The failure of the multivariate multifractal formalism

Section 4 provided a first and yet simple multifractal construction where the multivariate multifractal formalism developed in Section 3 fails to yield an upper bound for the multivariate multifractal spectrum (binomial cascades with $p < 1/2 < q$). This Section elaborates on the importance of *synchronicity* put forward in Section 3: First a pedagogical counter-example (bivariate scale-lacunary wavelet series) is devised that is designed to preclude synchronicity and hence to explain the origin and nature of the failure of the multivariate multifractal formalism (cf. Section 5(a)). Then a second example where the multivariate multifractal formalism fails (independent bivariate Lévy processes), better suited to real-world data modeling, is theoretically studied and numerically illustrated. Finally, the construction of a new multivariate multifractal formalism is proposed in Section 5(b). The theoretical general validity of this *cross-scale* formalism is proven, even when synchronicity is not assumed a priori.

(a) Counterexamples

(i) Scale-lacunary wavelet series

We consider a pair of lacunary "Weierstrass-type" wavelet series, for which the scales j_n^1 and j_n^2 of nonvanishing wavelet coefficients are farther and farther away from each other. Let $a > 1$ be the "lacunarity" parameter of the construction; the scales for which f_1 and f_2 have nonvanishing wavelet coefficients are respectively $j_n^1 = [a^{2n}]$ and $j_n^2 = [a^{2n+1}]$. Let $(\psi_{j,k})$ be a smooth orthonormal wavelet basis; we define

$$f_1(x) = \sum_{n=0}^{\infty} \sum_{k \in \mathbb{Z}} 2^{-\alpha j_n^1} \psi_{j_n^1,k}(x) \quad \text{and} \quad f_2(x) = \sum_{n=0}^{\infty} \sum_{k \in \mathbb{Z}} 2^{-\beta j_n^2} \psi_{j_n^2,k}(x). \tag{5.1}$$

As a direct consequence of the wavelet characterization of pointwise regularity,

$$\forall x \in \mathbb{R}, \qquad h_{f_1}(x) = \alpha \quad \text{and} \quad h_{f_2}(x) = \beta,$$

so that the joint multifractal spectrum of (f_1, f_2) is reduced to the point (α, β) where it takes the value 1 (and it is equal to $-\infty$ everywhere else).

   We now estimate the corresponding structure functions. The largest contributions to the structure functions are obtained when the leaders are either the largest (for r_1 or $r_2 > 0$) or the smallest (for r_1 or $r_2 < 0$). Thus, they are the largest for $j = j_n^1$ or j_n^2, and they are the smallest for $j = j_n^1 + 1$ or $j_n^2 + 1$ (so that we can limit the computation of structure functions to these cases).

- At scale j_n^1, there are $2^{j_n^1}$ wavelet leaders d_λ^1 of size $2^{-\alpha j_n^1}$ and $2^{j_n^1}$ leaders d_λ^2 of size $2^{-\beta j_n^2} \sim 2^{-\beta a j_n^1}$ (where $\sim$ means that the terms are equal up to factors that do not depend on the scales, but may depend on $a, \alpha, \beta,...$). Therefore

$$S(r_1, r_2, j_n^1) \sim 2^{-j_n^1} \sum_{\lambda \in \Lambda_{j_1}} 2^{-\alpha r_1 j_n^1} 2^{-\beta a r_2 j_n^1} \sim 2^{-(\alpha r_1 + \beta a r_2) j_n^1}.$$

- At scale $j_n^1 + 1$, there are $2^{j_n^1+1}$ wavelet leaders d_λ^1 of size $2^{-\alpha j_{n+1}^1} \sim 2^{-\alpha a^2 j_n^1}$ and $2^{j_n^1+1}$ leaders d_λ^2 of size $2^{-\beta j_n^2} \sim 2^{-\beta a j_n^1}$, so that

$$S(r_1, r_2, j_n^1 + 1) \sim 2^{-j_n^1-1} \sum_{\lambda \in \Lambda_{j_1}} 2^{-\alpha a^2 r_1 j_n^1} 2^{-\beta a r_2 j_n^1} \sim 2^{-(\alpha a^2 r_1 + \beta a r_2) j_n^1}.$$

- At scale j_n^2, there are $2^{j_n^2}$ leaders d_λ^1 of size $2^{-\alpha j_{n+1}^1} \sim 2^{-\alpha a j_n^2}$ and $2^{j_n^2}$ wavelet leaders d_λ^2 of size $2^{-\beta j_n^2}$, so that

$$S(r_1, r_2, j_n^2) \sim 2^{-j_n^2} \sum_{\lambda \in \Lambda_{j_1}} 2^{-\alpha r_1 a j_n^2} 2^{-\beta r_2 j_n^2} \sim 2^{-(\alpha r_1 a + \beta r_2) j_n^2}.$$

- At scale $j_n^2 + 1$, there are $2^{j_n^2+1}$ wavelet leaders d_λ^1 of size $2^{-\alpha j_{n+1}^1} \sim 2^{-\alpha a j_n^2}$ and $2^{j_n^2+1}$ leaders d_λ^2 of size $2^{-\beta j_{n+1}^2} \sim 2^{-\beta a^2 j_n^2}$, so that

$$S(r_1, r_2, j_n^2 + 1) \sim 2^{-j_n^2-1} \sum_{\lambda \in \Lambda_{j_1}} 2^{-\alpha r_1 a j_n^2} 2^{-\beta a^2 r_2 j_n^2} \sim 2^{-(\alpha r_1 a + \beta a^2 r_2) j_n^2}.$$

Thus the Legendre spectrum $L(H_1, H_2)$ is the characteristic function of the quadrilateral defined by the four points $(\alpha, \beta a)$, $(\alpha a^2, \beta a)$, $(\alpha a, \beta)$, $(\alpha a, \beta a^2)$. The point (α, β) (which is the support of the multifractal spectrum) is not included in it. Therefore, in this case, the Legendre spectrum does not yield an upper bound for the multifractal spectrum (their supports are even disjoint).

(ii) Lévy processes

We now perform the bivariate multifractal analysis of two independent Lévy processes. Let X_t be a Lévy process with no Brownian component, and denote by β its upper index of Blumenthal and Getoor (which in the case of stable processes, coincides with the selfsimilarity exponent), then the multifractal spectrum of a.e. sample path is

$$D(H) = \begin{cases} \beta H & \text{if } H \in [0, 1/\beta] \\ -\infty & \text{else,} \end{cases} \tag{5.2}$$

see [23]. Lévy processes are examples of processes where the irregularity sets $E^-(H)$ have the large intersection property, see [28]; the next result follows from this remark.

Corollary 5.1. *Let X_t^1 and X_t^2 be two independent Lévy processes of upper indices respectively β_1 and β_2; then the joint spectrum of a.e. couple of sample paths satisfies*

$$D^{\le}(H_1, H_2) = \begin{cases} \min(\beta_1 H_1, \beta_2 H_2) & \text{if } (H_1, H_2) \in [0, 1/\beta_1] \times [0, 1/\beta_2] \\ -\infty & \text{else.} \end{cases}$$

The Legendre spectra of each Lévy process satisfy (5.2), and the assumptions under which (6.1) holds are verified, so that the codimension formula holds, and

$$L(H_1, H_2) = \begin{cases} \beta_1 H_1 + \beta_2 H_2 - d & \text{if } (H_1, H_2) \in [0, 1/\beta_1] \times [0, 1/\beta_2] \\ -\infty & \text{else.} \end{cases}$$

Therefore (3.10) fails. Additionally, since $E_1(H_1)$ and $E_2(H_2)$ are empty if $H_1 < 0$ or if $H_2 < 0$, $E^{\le}(0,0) = E(0,0)$, so that $D(0,0) = D^{\le}(0,0)$ and (3.9) also fails: In conclusion, independent Lévy processes constitute another example where the Legendre spectrum does not give an upper bound for the joint multifractal spectrum. Thus the multivariate multifractal formalism fails for these important classes of stochastic processes, commonly used in real-world data modeling. Fig. 3 illustrates this numerically and plots the bivariate multifractal spectrum $D^{\le}(H)$, the point $D(H = (0,0))$, the predicted Legendre spectrum and a numerical estimate of it: indeed, theory and estimate for $L(H)$ practically collapse but are not upper bounds for $D^{\le}(H)$ or $D(H = (0,0))$.
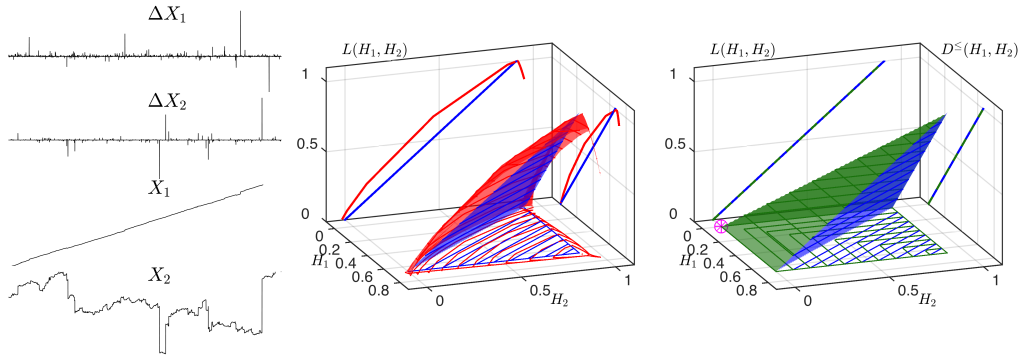
Figure 3. Multifractal analysis of independent Levy stable processes. Left: increments (ΔX_m) of sample paths (X_m) of two independent Levy processes time series ($M = 2$). Superposition of the predicted (blue) and estimated (red) Legendre spectra $L(H)$ (center), and of the theoretical bivariate multifractal spectrum $D^{\leq}(H)$ (green), the point $D(H = (0,0))$ (pink symbol) and the estimated Legendre spectrum $L(H)$ (red, right); the corresponding marginal spectra are plotted in the H_1 and H_2 planes. The numerical estimate of the Legendre spectrum $L(H)$ (in red) tightly follows the theoretical prediction (in blue), yet $L(H)$ is found to be below the multifractal spectrum $D^{\leq}(H)$ (in green). Even more, the support of $L(H)$ covers only half the support of $D^{\leq}(H)$ and misses the point $D(H = (0,0))$.

(b) Generalized cross-scale multivariate formalism

We have shown a major drawback of the multifractal formalism supplied by (3.8): In general, it does not yield an upper bound for the multifractal spectrum; it is the case when the exponents are synchronous, an assumption which, however, cannot be verified on real-life signals. This restriction raises the question of an alternative multifractal formalism which would yield in all generality an upper bound for the multivariate multifractal spectrum. The counterexamples that we studied clearly show that the multiresolution quantities that are used should incorporate leaders at different scales. The purpose of this section is to propose such quantities and show that the corresponding multifractal formalism satisfies the upper bound requirement that we mentioned. However, a full analytical and numerical analysis of this formalism would be far beyond the scope of the present paper and it will be performed in a future study.

We assume that $M = 2$. Here again extensions to arbitrary M are straightforward. The above counter-examples show that the problem with the structure functions (3.5) is that they "couple" leaders at the same scale only, thus missing possible interactions between different scales. A way to turn this drawback is to consider "richer" structure functions in which the couplings between leaders at different scales are incorporated. Note however that the coupling should be done between leaders that contribute to singularities at the same point. Thus, it has to be restricted to couples (λ_1, λ_2) of dyadic cubes such that one is included in the other. A first possibility is to consider structure functions of the following form: Suppose that $j_1 \leq j_2$; then

$$T(r_1, r_2, j_1, j_2) = 2^{-dj_2} \sum_{\lambda_1 \in \Lambda_{j_1}} \sum_{\lambda_2 \in \Lambda_{j_2} \text{ and } \lambda_2 \subset \lambda_1} |d^1_{\lambda_1}|^{r_1} |d^2_{\lambda_2}|^{r_2}. \tag{5.3}$$

However, these structure functions depend on the two scales j_1 and j_2; therefore their order of magnitude cannot be derived through a single log-log plot regression. One way to turn this problem is to come back to the starting point of the derivation of the multifractal formalism: If a point x belongs to $E(H_1, H_2)$, then, there exist an infinite number of scales j_1, j_2 such that $d^1_{\lambda_1} \approx 2^{-H_1 j_1}$ and $d^2_{\lambda_2} \approx 2^{-H_2 j_2}$, so that,

$$|d^1_{\lambda_1}|^{r_1} |d^2_{\lambda_2}|^{r_2} \approx 2^{-H_1 r_1 j_1} 2^{-H_2 r_2 j_2}. \tag{5.4}$$

One way to transform this two-scales relationship into a single-scale relationship is therefore to replace $d^1_{\lambda_1}$ by $(d^1_{\lambda_1})^{j_2/j_1}$, which yields $|d^1_{\lambda_1}|^{r_1 j_2/j_1} |d^2_{\lambda_2}|^{r_2} \approx 2^{-(H_1 r_1 + H_2 r_2) j_2}$, and new structure

functions for which one can draw log-log plot regressions versus j_2 only,

$$\text{if } j_1 \le j_2, \qquad S(r_1, r_2, j_1, j_2) = 2^{-dj_2} \sum_{\lambda_1 \in \Lambda_{j_1}} \sum_{\lambda_2 \in \Lambda_{j_2} \text{ and } \lambda_2 \subset \lambda_1} |d^1_{\lambda_1}|^{r_1 j_2/j_1} |d^2_{\lambda_2}|^{r_2}; \qquad (5.5)$$

it is further natural to symmetrize the formula by switching the roles of j_1 and j_2 which yields

$$\tilde{S}(r_1, r_2, j_1, j_2) = 2^{-dj_2} \sum_{\lambda_1 \in \Lambda_{j_1}} \sum_{\lambda_2 \in \Lambda_{j_2} \text{ and } \lambda_2 \subset \lambda_1} |d^1_{\lambda_2}|^{r_1} |d^2_{\lambda_1}|^{r_2 j_2/j_1}.$$

The corresponding *scaling function* is

$$\eta(r_1, r_2) = \lim_{\substack{(j_1, j_2) \to +\infty \text{ and } j_1 \le j_2}} \inf \frac{\log \left(S(r_1, r_2, j_1, j_2) + \tilde{S}(r_1, r_2, j_1, j_2) \right)}{\log(2^{-j_2})}. \qquad (5.6)$$

The *cross-scale Legendre spectrum* is obtained through a 2-variable Legendre transform

$$\forall (H_1, H_2) \in \mathbb{R}^2, \qquad \mathcal{L}(H_1, H_2) = \inf_{(r_1, r_2) \in \mathbb{R}^2} (d - \eta(r_1, r_2) + H_1 r_1 + H_2 r_2). \qquad (5.7)$$

Note that $\eta(r_1, r_2) \le \zeta(r_1, r_2)$ because the $\liminf$ in the definition of ζ is taken on a smaller set (the scales such that $j_1 = j_2$). It follows that $L(H_1, H_2) \le \mathcal{L}(H_1, H_2)$. Proposition 5.2 below shows that, in contradistinction with the Legendre spectrum (3.8), $\mathcal{L}(H_1, H_2)$ yields an upper bound for $D(H_1, H_2)$.

Proposition 5.2. *For any couple $(h_1(x), h_2(x))$ of exponents satisfying* (3.4),

$$\forall (H_1, H_2) \qquad D(H_1, H_2) \le \mathcal{L}(H_1, H_2). \qquad (5.8)$$

Proof: Let (H_1, H_2) be fixed, and let $\varepsilon > 0$. For $j_1, j_2 \ge 0$, we denote by $F(H_1, H_2, j_1, j_2, \varepsilon)$ the subset of $\Lambda_{j_1} \times \Lambda_{j_2}$ defined by the conditions

$$\lambda_2 \subset \lambda_1, \quad 2^{(-H_1-\varepsilon)j_1} \le d_{\lambda_1} \le 2^{(-H_1+\varepsilon)j_1} \quad \text{and} \quad 2^{(-H_2-\varepsilon)j_2} \le d_{\lambda_2} \le 2^{(-H_2+\varepsilon)j_1}; \qquad (5.9)$$

and we denote by $N(H_1, H_2, j_1, j_2, \varepsilon)$ the cardinality of this set. By restricting the sum in (5.5) to the elements of $F(H_1, H_2, j_1, j_2, \varepsilon)$, and using (5.9) it follows that

$$\forall r_1, r_2 \in \mathbb{R}, \qquad 2^{-dj_2} N(H_1, H_2, j_1, j_2, \varepsilon) 2^{-(r_1 H_1 + \varepsilon |r_1|) j_2} 2^{-(r_2 H_2 + \varepsilon |r_2|) j_2} \le S(r_1, r_2, j_1, j_2);$$

and from (5.6) we obtain that, for j_1 and j_2 large enough, $S(r_1, r_2, j_1, j_2) \le 2^{-j_2 (\eta(r_1, r_2) - \varepsilon)}$; thus

$$N(H_1, H_2, j_1, j_2, \varepsilon) \le 2^{j_2 (d - \eta(r_1, r_2) + \varepsilon + r_1 H_1 + \varepsilon |r_1| + r_2 H_2 + \varepsilon |r_2|)}. \qquad (5.10)$$

It follows from (3.4) that, if $x \in E(H_1, H_2)$, then x belongs to an infinite number of cubes λ_2 such that $(\lambda_1, \lambda_2) \in F(H_1, H_2, j_1, j_2, \varepsilon)$ (indeed $\lambda_2 \subset \lambda_1$, so that x also belongs to λ_1). If we denote by $G(H_1, H_2, j_1, j_2, \varepsilon)$ the collection of these cubes λ_2, then its cardinality also is $N(H_1, H_2, j_1, j_2, \varepsilon)$; thus, if $x \in E(H_1, H_2)$, then

$$\forall \varepsilon > 0, \qquad x \in \limsup_{j_1, j_2 \to +\infty} G(H_1, H_2, j_1, j_2, \varepsilon).$$

Thus,

$$\forall J_1 > 0, \qquad E(H_1, H_2) \subset \bigcup_{j_2 \ge j_1 \ge J_1} G(H_1, H_2, j_1, j_2, \varepsilon).$$

Let $A = d - \eta(r_1, r_2) + \varepsilon + r_1 H_1 + \varepsilon |r_1| + r_2 H_2 + \varepsilon |r_2|$; because of (5.10), $G(H_1, H_2, j_1, j_2, \varepsilon)$ is composed of less than 2^{Aj_2} dyadic cubes of width 2^{-j_2}. We use these cubes as ε-covering of

$E(H_1, H_2)$ and we obtain

$$\sum_{j_2 \geq j_1 \geq J_1} \sum_{(\lambda_1, \lambda_2) \in G(H_1, H_2, j_1, j_2, \varepsilon)} 2^{Aj_2} (2^{-j_2})^{\delta} \leq \sum_{j_2 \geq J_1} (j_2 - J_1 + 1) 2^{(A-\delta)j_2}$$

which is finite as soon as $\delta > A$. It follows that the Hausdorff dimension of $E(H_1, H_2)$ is bounded by $d - \eta(r_1, r_2) + \varepsilon + r_1 H_1 + \varepsilon|r_1| + r_2 H_2 + \varepsilon|r_2|$. Since this is true $\forall \varepsilon > 0$, $D(H_1, H_2)$ is bounded by $d - \eta(r_1, r_2) + r_1 H_1 + r_2 H_2$. Since this holds for any couple (r_1, r_2), the theorem is proved.

Note that (2.8) yields another upper bound for the bivariate spectrum. Therefore (5.7) is of interest only if it yields a sharper upper bound.

Proposition 5.3. *If the d_λ are bounded, then, for any couple of data,*

$$\mathcal{L}(H_1, H_2) \leq \min(L_1(H_1), L_2(H_2)), \tag{5.11}$$

and in general both quantities differ.

Proof: If $d_\lambda^1 \leq C$, then

$$S(r_1, r_2, j_1, j_2) \leq C 2^{-dj_2} \sum_{\lambda_1 \in \Lambda_{j_1}} \sum_{\lambda_2 \in \Lambda_{j_2} \text{ and } \lambda_2 \subset \lambda_1} |d_{\lambda_2}^2|^{r_2} = C 2^{-dj_2} \sum_{\lambda_2 \in \Lambda_{j_2}} |d_{\lambda_2}^2|^{r_2} = S_2(r_2, j_2).$$

It follows that $\eta(r_1, r_2) \geq \eta_2(r_2)$, so that $\mathcal{L}(H_1, H_2) \leq L_2(H_2)$. the same argument with $\tilde{S}$ yields that $\tilde{S}(r_1, r_2, j_1, j_2) \leq S_1(r_1, j_1)$, from which we conclude that $\mathcal{L}(H_1, H_2) \leq L_1(H_1)$, and hence (5.11) by exchanging the roles of H_1 and H_2.

We now give an example showing that this new formalism can yield a sharper upper bound than the trivial one supplied by $\min(L_1(H_1), L_2(H_2))$. We consider the interval $[0, 1]$, and define the d_λ^1 and d_λ^2 by

- If $\lambda \subset [0, 1/2]$ then $d_\lambda^1 = 2^{-\alpha_1 j}$ and $d_\lambda^2 = 2^{-\alpha_2 j}$.
- If $\lambda \subset [1/2, 1]$ then $d_\lambda^1 = 2^{-\beta_1 j}$ and $d_\lambda^2 = 2^{-\beta_2 j}$.

Then $S(r_1, r_2, j_1, j_2) = \frac{1}{2} \left(2^{-(\alpha_1 r_1 + \alpha_2 r_2)j_2} + 2^{-(\beta_1 r_1 + \beta_2 r_2)j_2} \right)$. It follows that the scaling function is $\eta(r_1, r_2) = \min(\alpha_1 r_1 + \alpha_2 r_2, \beta_1 r_1 + \beta_2 r_2)$, and its Legendre transform $\mathcal{L}(H_1, H_2)$ is the characteristic function of the segment of ends (α_1, α_2) and (β_1, β_2). This is to be compared with the trivial bound supplied by (5.11) which, in this case is the characteristic function of the rectangle delimited by the four points (α_1, α_2), (α_1, β_1), (β_1, α_2), (β_1, β_2) (we compare the diagonal of the rectangle with the rectangle itself).

6. Interpreting the multivariate multifractal and Legendre spectra

Of central interest in multivariate multifractal analysis is to understand which information the shape of a multivariate multifractal spectrum yields on data, and on the relationships between their different components. Again, the discussion is conducted in a bivariate setting for simplicity, but extends straightforwardly to $M \geq 2$. By definition, the multifractal spectrum $D(H_1, H_2)$ quantifies the co-occurences of Hölder exponents taking jointly values H_1 for component 1 and H_2 for component 2. This holds both for deterministic functions and sample paths of stochastic processes. The interpretation of the Legendre spectrum $L(H_1, H_2)$ requires more attention and can be discussed along two lines: synchronicity vs. non synchronicity and, in a stochastic process setting, dependence vs. independence.

Remark: *In [29], for a function $f : \mathbb{R}^d \to \mathbb{R}$, a comparison between the (wavelet) large deviations spectrum and the multifractal spectrum was used to detect the presence of oscillating singularities for f. It is certainly*

worth investigating whether some similar conclusions could be obtained for multivariate functions, i.e. what conclusions can be deduced from the non-coincidence between the multifractal, the large deviations and the Legendre spectra.

(a) Synchronicity vs. non synchronicity

When the synchronicity assumption (cf. Section 3) is satisfied, the Legendre spectrum $L(H_1, H_2)$ yields an upper bound of $D(H_1, H_2)$. The interpretation as cooccurrence of Hölder exponents associated with $D(H_1, H_2)$ thus also holds for $L(H_1, H_2)$.

When the synchronicity assumption is not satisfied, the interpretation of $L(H_1, H_2)$ must be weakened as follows. The wavelet leaders $(d_\lambda^1, d_\lambda^2)$ associated with the sample paths of the two components can be seen as random variables whose distributions are controlled by the *bivariate large deviation spectrum*: $\mathcal{D}(H_1, H_2) \triangleq \lim_{\epsilon \to 0} \limsup_{j \to \infty} N_j(H_1, H_2, \varepsilon)$, where $N_j(H_1, H_2, \varepsilon) =$ card $\left\{ \lambda \in \Lambda_j : \quad H_1 - \varepsilon \leq \ell_j(d_\lambda^1) \leq H_1 + \varepsilon \quad \text{and} \quad H_2 - \varepsilon \leq \ell_j(d_\lambda^1) \leq H_2 + \varepsilon \right\}$. Indeed, $\mathcal{D}(H_1, H_2)$ quantifies the number of couples $(d_\lambda^1, d_\lambda^2)$ such that jointly $d_\lambda^1 \sim 2^{-H_1 j}$ and $d_\lambda^2 \sim 2^{-H_2 j}$.

The univariate relationship between the large deviation spectrum and the Legendre spectrum can be extended to the multivariate setting, and states that $L(H_1, H_2)$ is the concave hull of $\mathcal{D}(H_1, H_2)$. Therefore, if the large deviation spectrum is concave, the Legendre spectrum $L(H_1, H_2)$ can be given the interpretation of cooccurrences of the multiscale quantities $(d_\lambda^1, d_\lambda^2)$. These discussions and interpretations are to be understood sample-path wise and are thus valid both in deterministic and stochastic settings. Note that techniques to estimate large deviations spectra have recently been developed, see [30] and ref. therein.

(b) Legendre spectrum in a stochastic setting

(i) Stationarity and independence

To gain insights into the properties of the multivariate Legendre spectrum in a stochastic setting, let us consider bivariate stochastic processes, with stationary wavelet coefficients at each scale. This is for instance the case for stationary processes, or processes with increments of a given order that are stationary. Under stationarity of the wavelet coefficients, the structure functions defined in (3.5) can be interpreted as sample moment estimators of the random variables d_λ

$$S(r_1, r_2, j) = 2^{-dj} \sum_{\lambda \in \Lambda_j} |d_\lambda^1|^{r_1} |d_\lambda^2|^{r_2} \sim \mathbb{E}\left(|d_\lambda^1|^{r_1} |d_\lambda^2|^{r_2} \right).$$

Further, assuming independence of the components, the wavelet coefficients and wavelet leaders d_λ^1 and d_λ^2 are also independent, yielding $S(r_1, r_2, j) \sim \mathbb{E}(|d_\lambda^1|^{r_1}) \mathbb{E}(|d_\lambda^2|^{r_2})$ and hence $S(r_1, r_2, j) = S^1(r_1, j) S^2(r_2, j)$.

Assuming that the liminf in (3.6) is a true limit, the assumption of stationarity and independence thus leads to $\zeta(r_1, r_2) = \zeta^1(r_1) + \zeta^2(r_2)$ and (3.8) becomes

$$
\begin{aligned}
L(H_1, H_2) &= \inf_{(r_1, r_2) \in \mathbb{R}^2} (d - \zeta^1(r_1) + \zeta^2(r_2) + H_1 r_1 + H_2 r_2) \\
&= \inf_{r_1} (d - \zeta^1(r_1) + H_1 r_1) + \inf_{r_2} (d - \zeta^2(r_2) + H_2 r_2) - d,
\end{aligned}
$$

which leads to

$$L(H_1, H_2) = L(H_1) + L(H_2) - d. \tag{6.1}$$

This derivation follows the one proposed in [6], rewritten in the framework of multiscale quantities, and shows that under the joint assumptions of stationarity and independence, the codimension rule (2.9) applies for the multivariate Legendre spectrum. This is valid irrespective of whether synchronicity holds or not. A practical outcome is that any departure of the Legendre spectrum from (6.1) indicates that either of the assumptions (stationarity or independence) required to yield (6.1) does not hold.

(ii) Dependence vs. independence

Let us now discuss the relations between the shape of $L(H_1, H_2)$ and statistical dependencies. We first assume stationarity of the multiscale quantities. It has been documented in [6], using a formalism dedicated to measures, that the dependence amongst components of cascades controls the shape of the corresponding bivariate Legendre spectrum, that is, the departures of $L(H_1, H_2)$ from $L(H_1) + L(H_2) - d$. Elaborating on these results, and using a wavelet leader-based multifractal formalism, it has further been shown and illustrated that the higher-order statistical dependencies amongst components of a bivariate multifractal random walk also control the bivariate Legendre spectrum [16,17]. More generally, let μ_1 and μ_2 denote two non-atomic stationary probability measures on $[0, 1]$ (as in [31,32]) with pointwise correlation ρ_{MF}, and let F_1 and F_2 be their respective cumulative density functions (i.e. $F(x) = \mu[0, x]$). These results suggest that $L_{F_1, F_2}(H_1, H_2) \neq L_{F_1}(H_1) + L_{F_2}(H_2) - d$, and this deviation of $L_{F_1, F_2}(H_1, H_2)$ from $L_{F_1}(H_1) + L_{F_2}(H_2) - d$ is due to the dependence of μ_1 and μ_2 that is controlled by ρ_{MF}.

We now drop the stationarity assumption for μ_1 and μ_2; being continuous and monotonously increasing functions, F_1 and F_2 can be used as a *time-change* for stochastic processes, and permit to extend this discussion to bivariate fractional Brownian motions in multifractal time, as defined in [33] in a univariate setting. Let B_α and B_β denote two fractional Brownian motions, with exponents α and β, with pointwise correlation ρ_{SS}. Then, we construct $\mathcal{B}_{\alpha, \mu_1}(t) = B_\alpha(F_1(t))$ and $\mathcal{B}_{\beta, \mu_2}(t) = B_\alpha(F_2(t))$, whose pointwise correlation ρ is a function of both ρ_{MF} and ρ_{SS}. For functions or processes whose Hölder exponents take values in $[0, 1]$, or for which the polynomial in (2.1) always consists of a constant, standard uniform estimates on increments of fBm yield

$$\text{a.s.} \quad \forall x_0, \ h_{B_\alpha(X)}(x_0) = \alpha h_X(x_0), \tag{6.2}$$

see e.g. [33]. It follows that, a.s.:

$$D_{\mathcal{B}_{\alpha, \mu_1}}(H) = D_{F_1}\left(\frac{H}{\alpha}\right), \quad D_{\mathcal{B}_{\beta, \mu_2}}(H) = D_{F_2}\left(\frac{H}{\beta}\right)$$

$$D_{\mathcal{B}_{\alpha, \mu_1}, \mathcal{B}_{\beta, \mu_2}}(H_1, H_2) = D_{F_1, F_2}\left(\frac{H_1}{\alpha}, \frac{H_2}{\beta}\right), \tag{6.3}$$

$$\text{and} \quad L_{\mathcal{B}_{\alpha, \mu_1}, \mathcal{B}_{\beta, \mu_2}}(H_1, H_2) = L_{F_1, F_2}\left(\frac{H_1}{\alpha}, \frac{H_2}{\beta}\right). \tag{6.4}$$

This illustrates the following key features of the multifractal and Legendre spectra that are valid generically in a stochastic setting. The shapes of the bivariate multifractal and Legendre spectra are independent of the correlation ρ_{SS}; further, they depend on the parameters α and β of the fractional Brownian motions B_α and B_β only trivially, by contraction along the H_1 and H_2 axes of the marginal and thus the joint spectra. Any non-trivial deformation of the spectra is hence due to dependence not quantified by correlation: In other words, the bivariate multifractal and Legendre spectra yield information on *higher order statistical dependencies* amongst components, beyond the correlation coefficient. For example, $\rho_{SS} \equiv 0$ obviously implies $\rho \equiv 0$, while the bivariate Legendre spectrum can be tuned by ρ_{MF} from $L_{\mathcal{B}_{\alpha, \mu_1}, \mathcal{B}_{\beta, \mu_2}}(H_1, H_2) \equiv L_{F_1}(\frac{H_1}{\alpha}) + L_{F_2}(\frac{H_2}{\beta}) - 1$ when $\rho_{MF} \equiv 0$ to $L_{\mathcal{B}_{\alpha, \mu_1}, \mathcal{B}_{\beta, \mu_2}}(H_1, H_2) \equiv L_{F_1}(\frac{H_1}{\alpha}) 1_{H_1 \pm \alpha H_2/\beta}$ when $\rho_{MF} \equiv \pm 1$, independently of ρ_{SS}. Therefore, the existence of higher order statistical dependencies beyond correlation amongst components do induce and control departures of $L(H_1, H_2)$ from the codimension rule prediction: $L(H_1) + L(H_2) - 1$.

However, and counterintuitively, the converse is not necessarily true, as can be shown from the following example. Let $\mu_1 \equiv \mu_2 \equiv \mu$ and hence $F_1 = F_2 \equiv F \equiv \mu[0, x]$. Let B_α and B_β denote two independent fBm, with exponents α and β. Then, by construction, the compound processes $\mathcal{B}_{\alpha, \mu}(t) = B_\alpha(F(t))$ and $\mathcal{B}_{\beta, \mu}(t) = B_\beta(F(t))$ are independent. However, their bivariate Legendre spectrum obviously reads $L_{\mathcal{B}_{\alpha, \mu}, \mathcal{B}_{\beta, \mu}}(H_1, H_2) \equiv L_F(\frac{H_1}{\alpha}) 1_{H_1 = \alpha H_2/\beta}$ and hence departs from the co-dimension formula. This is illustrated in Fig. 4 using the binomial cascades (μ_p, μ_q) with $0 < p, q < 1/2$ defined in Section 4 and $\alpha = \beta = 1/2$.
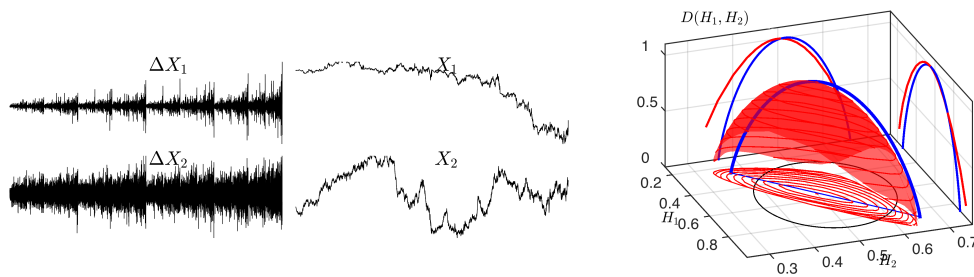
Figure 4. Multifractal analysis of Brownian motion in multifractal time. Left: Increments (ΔX_m) and sample paths (X_m) of bivariate Brownian motion compound with bivariate binomial cascades ($p_1, p_2 < 1/2$); Right: theoretical bivariate multifractal spectrum $D(H)$ (blue) and estimated Legendre spectrum $L(H)$ (red); the corresponding marginal spectra are plotted in the H_1 and H_2 planes. Although the two sample paths X_1 and X_2 are statistically independent, co-dimensions do not add up: The support of $D(H)$ collapses to a line segment in this case, and the estimate for $L(H)$ is in better agreement with $D(H)$ than with the ellipsoidal support of a spectrum obtained by adding up co-dimensions (indicated in black), which it fails to cover.

7. Conclusion

In [6], a natural multivariate extension of the univariate multifractal formalism was proposed, based on increments and in the context of hydrodynamic turbulence. Reformulating this multivariate formalism in the wavelet leader framework, as proposed in [13,14], enabled us to investigate its range of validity and to contribute a number of new insights and results:

i) The notions of synchronicity of multiscale quantities and minimizing sequences amongst data components demonstrates that under synchronicity the multivariate Legendre spectrum can be associated with co-occurences of singularities among components, and thus be formally related to the multivariate (Hausdorff) multifractal spectrum, as its upper bound ;

ii) The construction of counterexamples, both pedagogical or realistic with respect to real-world data, shows that the proposed multivariate extension of the univariate multifractal formalism is not valid if synchronicity fails: the multivariate Legendre spectrum can fail to provide an upper bound for the multivariate (Hausdorff) multifractal spectrum ;

iii) A mathematical foundation for a multivariate multifractal formalism which fulfills the upper bound requirement has been proposed and studied theoretically ;

iv) Interpretations and usefulness of the multivariate Legendre spectrum were discussed both in determinist and stochastic settings, in terms of synchronicity, stationarity and statistical dependencies.

The theoretical results were validated numerically by computing multivariate Legendre spectra from synthetic data using a *Multvariate Multifractal Analysis Toolbox* designed by ourselves that will made publicly available and documented at the time of publication. Future work will focus on addressing the practical issues related to the numerical implementation related with this generalized formalism.

References

1. S. Jaffard, Wavelet techniques in multifractal analysis, in: Fractal Geometry and Applications: A Jubilee of Benoît Mandelbrot, M. Lapidus and M. van Frankenhuijsen, Eds., Proc. Symposia

in Pure Mathematics, Vol. 72(2), AMS, 2004, pp. 91–152.

2. P. Abry, S. Jaffard, H. Wendt, Irregularities and scaling in signal and image processing: Multifractal analysis, Benoit Mandelbrot: A Life in Many Dimensions, M. Frame and N. Cohen, Eds., World scientific publishing (2015) 31–116.

3. S. Jaffard, C. Melot, R. Leonarduzzi, H. Wendt, S. G. Roux, M. E. Torres, P. Abry, p-exponent and p-leaders, Part I: Negative pointwise regularity, Physica A 448 (2016) 300–318.

4. R. Leonarduzzi, H. Wendt, S. G. Roux, M. E. Torres, C. Melot, S. Jaffard, P. Abry, p-exponent and p-leaders, Part II: Multifractal analysis. Relations to Detrended Fluctuation Analysis, Physica A 448 (2016) 319–339.

5. G. Parisi, U. Frisch, Fully developed turbulence and intermittency, in: M. Ghil, R. Benzi, G. Parisi (Eds.), Turbulence and Predictability in geophysical Fluid Dynamics and Climate Dynamics, Proc. of Int. School, North-Holland, Amsterdam, 1985, p. 84.

6. C. Meneveau, K. Sreenivasan, P. Kailasnath, M. Fan, Joint multifractal measures - theory and applications to turbulence, Physical Review A 41 (2) (1990) 894–913.

7. J. Peyrière, A vectorial multifractal formalism, Proc. Symp. Pure Math. 72.2 (2) (2004) 217–230.

8. L. Barreira, B. Saussol, J. Schmeling, Higher-dimensional multifractal analysis, J. Math. Pures Appl. 81 (2002) 67–91.

9. L. Olsen, Mixed generalized dimensions of self-similar measures, J. Math. Anal. Appl. 306 (2005) 516–539.

10. M. Morán, Problems on self-similar geometry, in: C. Bandt, S. Graf, M. Zähle (Eds.), Fractal Geometry and Stochastics II, Greifswald, Germany, August, 1998, Birkhäuser Verlag, 2000, p. 69–93.

11. L. Olsen, Mixed divergence points of self-similar measures, Indiana University Mathematics Journa 52 (2003) 1343–1372.

12. M. Morán, Multifractal components of multiplicative set functions, Math. Nachr. 229 (2001) 129–160.

13. S. Jaffard, S. Seuret, H. Wendt, R. Leonarduzzi, S. Roux, P. Abry, Multivariate multifractal analysis, Appl. Comput. Harm. Anal. 46 (3) (2019) 653–663.

14. M. Ben Slimane, Baire typical results for mixed Hölder spectra on product of continuous Besov or oscillation spaces, Mediterr. J. Math. 13 (2016) 1513–1533.

15. M. Ben Abid, Prevalent mixed Hölder spectra and mixed multifractal formalism in a product of continuous Besov spaces, Nonlinearity 30 (2017) 3332–3348.

16. H. Wendt, R. Leonarduzzi, P. Abry, S. Roux, S. Jaffard, S. Seuret, Assessing cross-dependencies using bivariate multifractal analysis, in: IEEE Int. Conf. Acoust., Speech, and Signal Proces. (ICASSP), Calgary, Canada, 2018.

17. R. Leonarduzzi, P. Abry, S. G. Roux, H. Wendt, S. Jaffard, S. Seuret, Multifractal characterization for bivariate data, in: Proc. European Signal Processing Conference (EUSIPCO), Rome, Italy, 2018.

18. P. Abry, S. Jaffard, R. Leonarduzzi, C. Melot, H. Wendt, New exponents for pointwise singularity classification, in: S. Seuret, J. Barral (Eds.), Recent Developments in Fractals and Related Fields: Proc. Fractals and Related Fields III, 19-26 September 2015, Porquerolles, France, 2017, pp. 1–37.

19. P. Mattila, Geometry of Sets and Measures in Euclidean Spaces: Fractals and Rectifiability, Cambridge Studies in Advanced Mathematics, 1999.

20. K. Falconer, Fractal Geometry: Mathematical Foundations and Applications, John Wiley & Sons, West Sussex, England, 1993.

21. A. Durand, Sets with large intersection and ubiquity, Mathematical Proceedings of the Cambridge Philosophical Society 144 (1) (2008) 119–144.

22. J. M. Aubry, S. Jaffard, Random wavelet series, Comm. Math. Phys. 227 (3) (2002) 483–514.

23. S. Jaffard, The multifractal nature of Lévy processes, Probability Theory and Related Fields 114 (2) (1999) 207–227.

24. L. Barreira, B. Saussol, Variational principles and mixed multivariate spectra, Trans. A. M. S. 353 (10) (2001) 3919–3944.

25. A.-H. Fan, D.-J. Feng, J. Wu, Recurrence, dimension and entropy, J. London Math. Soc. 11 (3) (2001) 229–244.

26. A. Arneodo, E. Bacry, S. Jaffard, J. Muzy, Singularity spectrum of multifractal functions involving oscillating singularities, J. Fourier analysis and Applications 4 (1998) 159–174.

27. B. B. Mandelbrot, Intermittent turbulence in self-similar cascades: divergence of high moments and dimension of the carrier, J. Fluid Mech. 62 (1974) 331–358.

28. A. Durand, Singularity sets of Lévy processes, Probab. Theory Relat. Fields 143 (2009) 517–544.
29. S. Seuret, Detecting and creating oscillations using multifractal methods, Math. Nachr. 279 (11) (2006) 1195–1211.
30. R. Leonarduzzi, P. Abry, H. Wendt, S. Jaffard, H. Touchette, A generalized multifractal formalism for the estimation of nonconcave multifractal spectra, IEEE T. Signal Proces. 67 (1) (2019) 110–119.
31. E. Bacry, J. Delour, J.-F. Muzy, Multifractal random walk, Phys. Rev. E 64: 026103 (2001).
32. J. Barral, B. Mandelbrot, Random multiplicative multifractal measures, Proc. Symp. Pures Math., M. L. Lapidus and M. van Frankenhuysen eds 72 (2004) 1–52.
33. B. Mandelbrot, Scaling in financial prices: III. cartoon Brownian motions in multifractal time, Quantitative finance 1 (2001) 427–440.